Magnus Styrker Eliassen

Model Tests and Numerical Analysis of Wave Loads on Coastal Structures

Master's thesis in Product and System Design
Supervisor: Henry Piehl, Vilmar Æsøy
June 2019

Master's thesis

◼ NTNU
**Norwegian University of
Science and Technology**

Magnus Styrker Eliassen

Model Tests and Numerical Analysis of Wave Loads on Coastal Structures

NTNU
Norwegian University of
Science and Technology

Abstract

This research investigates the effects of wave loads on coastal structures. With today's shifting focus towards clean and renewable energy, sources such as offshore wind turbines offer a promising potential. More specifically, the research is focusing on the cylindrical structure which the wind turbines are based on. The research aims to investigate what methods are most suited to develop a numerical test tank and how it can be used for simulation-based design of structures in waves.

To investigate the effect of wave loads on coastal structures, both numerical- and experimental methods were used. These methods were used to replicate a scenario where waves are washed against a cylindrical structure. The cylindrical structure is virtually developed and analyzed. Assessment of sensor performance for the experimental tests was done to ensure the credibility of the research. Since it is used multiple methods to obtain results, the parameters are as identical as possible. This limits the research to the capabilities and dimensions of the wave tank available for the scaled experimental tests. The numerical models are based on computational fluid dynamics and computer aided engineering.

The results from the research show that with the given parameters, the exerted wave force on a cylindrical structure is quite low. Both the numerical- and experimental models provide results that are in the same range. By getting similar results for different methods, the research shows that it has potential.

Preface

This report is the result of my Master's thesis in Product and System Design, completed in the spring of 2019. The thesis is written for the Department of Ocean Operations and Civil Engineering at The Norwegian University of Science and Technology (NTNU), located in Ålesund, Norway. It represents the end of my days as a student at NTNU Ålesund.

I want to take this opportunity to thank my family and friends for their support and belief in me. They were always there to help me in time of needs and to commemorate accomplishments together. A special thanks go out to my classmates who have made this journey unforgettable. We have spent countless hours together and shared both frustration and laughter. I could not have wished for a better environment than they have provided, these years would not have been the same without them. I wish them all, the best of luck in the future to come.

I would also like to express my gratitude towards my supervisor, Henry Piehl for insightful information and guidance throughout the thesis. Much of the work in the thesis was made possible by his help, especially regarding numerical models.

My co-supervisor, Vilmar Æsøy, also deserves recognition for his contribution and guidance to the practical aspect of the thesis. He has come with several useful suggestions to the model design and how to execute an experimental test.

Both of my supervisors have provided invaluable expertise in their respective fields that have contributed to the progress of this thesis. Thank you.

_____

Magnus Styrker Eliassen

Ålesund, June 2019

Table of Contents

List of Figures

List of Tables

List of Abbreviations

CFD	Computational Fluid Dynamics
FEM	Finite Element Method
PDE	Partial Differential Equations
FVM	Finite Volume Method
VOF	Volume of Fluids
DOF	Degrees of Freedom
GF	Gauge Factor

1 Introduction

1.1 Problem

With today's energy situation, the focus is shifting more and more towards clean and renewable energy. One such source that shows promising potential is offshore wind energy. The offshore wind energy is both clean and renewable. Offshore wind farms are usually located in shallow waters at depths of 5 to 30 m (IEE, 2018). The substructures used for the wind turbines are monopiles, tripods and truss towers. These cylindrical shaped structures are exposed to hydrodynamic loads from the intermediate and shallow water waves. With the increased development in wind farms, it is needed to have sufficient knowledge of the forces that are exerted from the waves hitting these coastal structures.

Acquiring the needed data to design the wind farms can be a troublesome process as there are numerous variables to take into consideration. The design of a coastal structure is based on thorough testing and validation. It also has to be taken into consideration how the data is going to be gathered. Simply building a wind turbine and placing it in the ocean to see what happens is a costly approach and run the risk of providing false, untrustworthy data. Another aspect that is difficult to measure is how the waves act around the cylindrical structure, not just at the impact point. A consequence of all the various input variables is that the results can be difficult to replicate or match against similar test cases. For the data to be used, some degree of validation is needed.

One of the variables that will be difficult to reenact are the waves hitting the coastal structures. What type of waves the cylindrical structures are exposed to will vary, depending on the seabed and the climate in the specific area. The test tank used for a small-scale test is set with fixed parameters, such as limitations regarding size and equipment. With inadequate equipment, the data will be inconsistent and unreliable. An example of this could be low-quality sensors. With the limitations of a wave tank, it will be challenging to match the results each time. How a wave dissipates in a wave tank will be different from a real-life scenario.

Figure 1.1 Examples of offshore wind turbines **(DNV GL, 2018)**

1.2 Motivation

Scaled test scenarios can be used to save both time and money when developing an offshore wind farm. A small-scale test can be arranged to near real-life conditions to provide a good indication of how the structure will behave when exposed to waves. It is also easier to simulate extreme conditions in a controlled environment to get the worst-case scenario results.

With more data gathered from scaled test versions, it is possible to compare the results against each other. Comparing results helps with validation for the tests conducted. As more and more test situations are analyzed the accuracy increases. A more accurate result will lead to better calibration for future testing and to help others that are interested in the topic. A good database also rules out test scenarios that provide false or untrustworthy data.

Along with scaled modeled testing a numerical approach can be used. By comparing the numerical approach with the experimental approach, results can be further validated. As with the various scaled testing scenarios, there are various ways of doing a numerical approach. However, it is the combined results for all the various approaches that should be used to establish a solid base of knowledge for the topic being investigated.

With an improved numerical simulation model, it is easier to design new experiments. The numerical approach could be based on several methods. Some of which might be simple calculations or computer-based tools such as Computational Fluid Dynamics (CFD) and Finite Element Method (FEM) analysis. All of which contributes to establishes a good base for new experiments.

1.3 Scope

There are several ways of approaching a topic regarding wave loads on coastal structures. How broad the investigation on the topic should be will be limited by time and what the goal with the work is. For the master thesis, it would be too of big a task to look at every aspect regarding wave loads on coastal structures. The thesis will therefore narrow it down to three main topics; Numerical methods, experimental tests and coastal structures. How much work will be put into each of the topics will vary.

Along with the time constraint, each of the topics will have limitations within themselves. This is done to direct the attention towards answering specific questions regarding the topic. One limitation will be the available equipment. The experimental tests will be conducted in a towing tank available at the university.
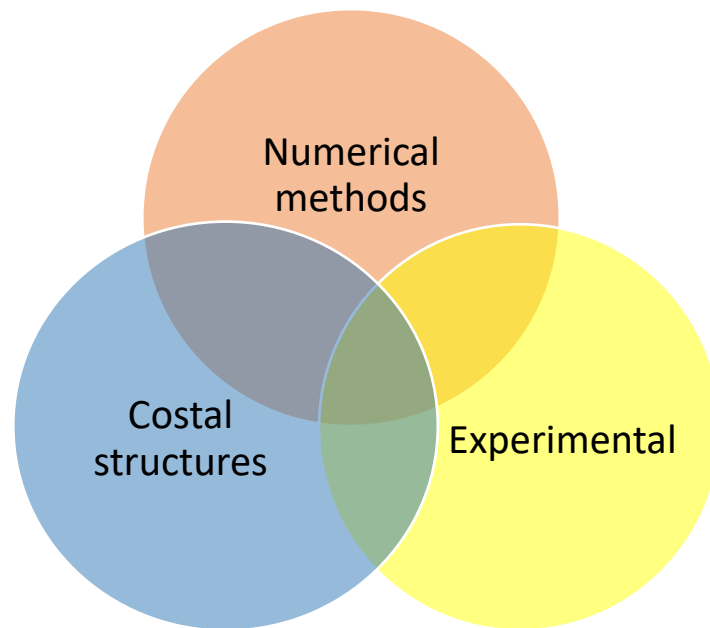
Figure 1.2 Scope

The investigation focuses on monopile structures since they are one of the most common coastal structure types. This means to investigate and test several loads on a single structure instead of a few loads on many structures. By choosing only one structure it also limits the shape to investigate. The monopile is shaped like a slender cylinder. The dimensions for the cylinder will be at a scaled ratio with a full-size wind turbine as a rough baseline.

The numerical analysis will include FEM and CFD. The goal of using these tools is to establish a numerical simulation framework, combining both structural FEM and hydrodynamic CFD calculations.

Experimental testing will be limited to a single structure. This way, there is less room for error and a consistent result can be achieved. A goal for the tests performed in the tank is to get a consistency of waves. To measure the waves hitting the cylindrical structure it is to be fitted with sensors.

1.4 Objective

The objective of the thesis is to investigate the effects of wave loads on coastal structures via numerical analysis with model testing validation. A combination of the methods will ensure the validity of the results, opening the possibility of quickly designing new similar experiments. To understand the wave load effects on a coastal structure, several approaches can be used. A numerical approach would be a good place to start when analyzing a monopile structure.

Since the various approaches are dependent on each other, the thesis will be a somewhat iterative process. For the tests to be compared against each other, the parameters have to be the same. Also, while it is easy to change dimensions in a numerical test, redesigning the experimental test is a more demanding process. One of the things that need to be determined is the thickness of the cylinder. If this is too thick, the experimental tests may not yield any results due to the sensor not registering any data.

The thesis will therefore start by doing numerical analysis on the structure. With the parameters finalized, the experimental test is to be conducted. The experimental test will be done in the towing tank available at the university. By gathering data from the scaled monopile structure, it is possible to verify the numerical results. If the experimental and numerical results match, it is possible to validate the testing methods allowing for a better calibration of a numerical simulation model.

Figure 1.3 Towing tank to be used in experimental tests

Research questions:

- What methods are most suited to develop a numerical test tank?

- How can the numerical test tank be used for simulation-based design of structures in waves?

- Assessment of sensor performance and virtual development procedure.

1.5 Approach

As the title states, the thesis will use both numerical- and experimental methods to achieve its goal. The thesis will develop a numerical method for analyzing wave loads on coastal structures. This will involve both simple calculations and using computer-based engineering tools to establish a numerical model. The main computer-based engineering tools will be finite element method and computational fluid dynamics. These tools analyze the results by using different methods, ensuring that the problem is being investigated from various perspectives. To validate these results, a scaled model test will be performed in a towing tank. This will give validation to the research.

The thesis will start by gathering the necessary information that could be useful in the research. Some of this work has been done in the literature chapter. It is also needed to have some requirements set for the cylindrical structure that is to be modeled both numerically and experimentally. The most important requirements will be regarding the structural size. It will be essential to get a good scaling value from an actual wind turbine monopile.

With the essential information and requirements known, it is possible to start on the analytical- and numerical models of the structure. The analytical model will be calculations based on a standard beam structure. From this, it is possible to start simulating with the finite element method. By applying the wave force, it can be determined if the geometry of the structure is sufficient or not. With a structural proposal, the fluid flow can be simulated by using computational fluid dynamics. This will indicate how the fluid behaves around the structure. It is important to note that this will be an iterative process and that several designs will be tested.

To validate the numerical models, a scaled model test will be done in the wave tank available at the school. An important aspect with the experimental testing is the sensors used to register the forces exerted from the waves. If the wall thickness of the cylinder is too thick the sensors might be too weak to register any data. Correct geometry and suitable sensors are therefore a necessity with the experimental testing. To get consistency from the results, the testing will be based on a single structure for both methods used.
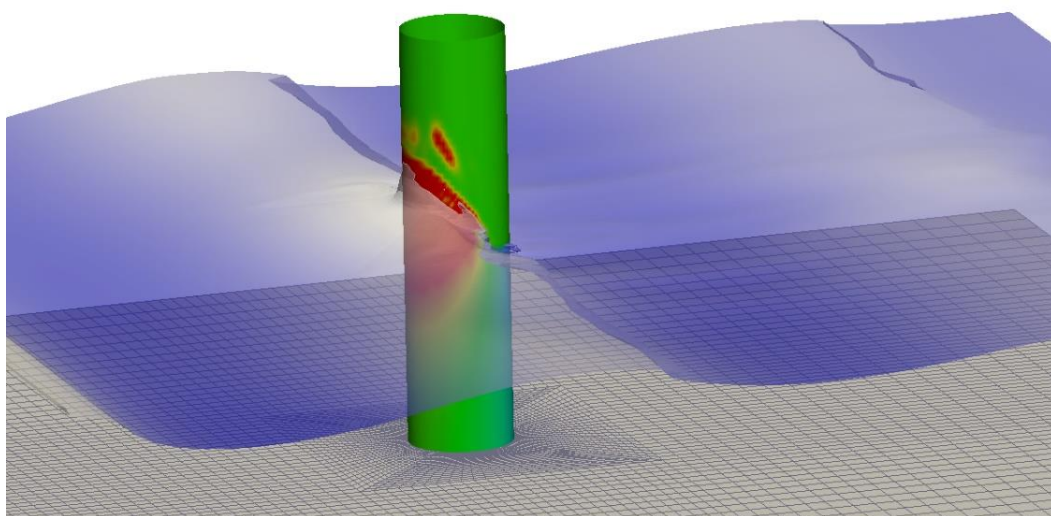
Figure 1.4 Illustration of problem to be solved **(Piehl, 2018)**

2 Literature review

2.1 Coastal structures

2.1.1 Generic on coastal structures

Coastal structures are usually installed for the purpose of producing or transporting electricity, oil, gas and other resources. This goes under the term maritime engineering. There are various types of structures used for different purposes. The various type of structures can be floating, moored to the seabed, fixed to the seabed or completely subsea.

Figure 2.1 Examples on offshore structures **(NTNU, 2018)**

Figure 2.1 shows a broad example of what can be considered as offshore structures. While the term offshore structure is a somewhat more extensive term than coastal structure, it gives a good indication of what can be considered as coastal structures.

2.1 Coastal structures

Each of the coastal structures shown in Figure 2.1 serves a specific function within the maritime industry. One more element that could be added to the figure is coastal wind farms. Ever since the first oil rig was producing oil back in 1897, (American Oil & Gas Historical Society, 2014) the maritime industry has had an enormous growth. Over the years the industry has found new methods of extracting resources and improved on the existing technologies. Some of the improvements new technologies and methods have contributed to is the depth at which resources can be extracted. The most extreme drilling rigs operate at ultra-Deepwater, reaching drilling depths of over 9000 m (Transocean, 2018). An alternative to the traditional platform rigs is the submerged subsea production systems. This solution provides a way to produce hydrocarbons from areas not economically or easily developed by using a traditional platform rig (AkerSolutions, 2018).

The maritime industry is responsible for several resources that are essential in today's society. However, in recent times the focus has shifted towards renewable and clean resources. This is why coastal wind farms have become more and more popular. This is both a clean and renewable way to extract energy. It is also possible to do this for ocean currents.
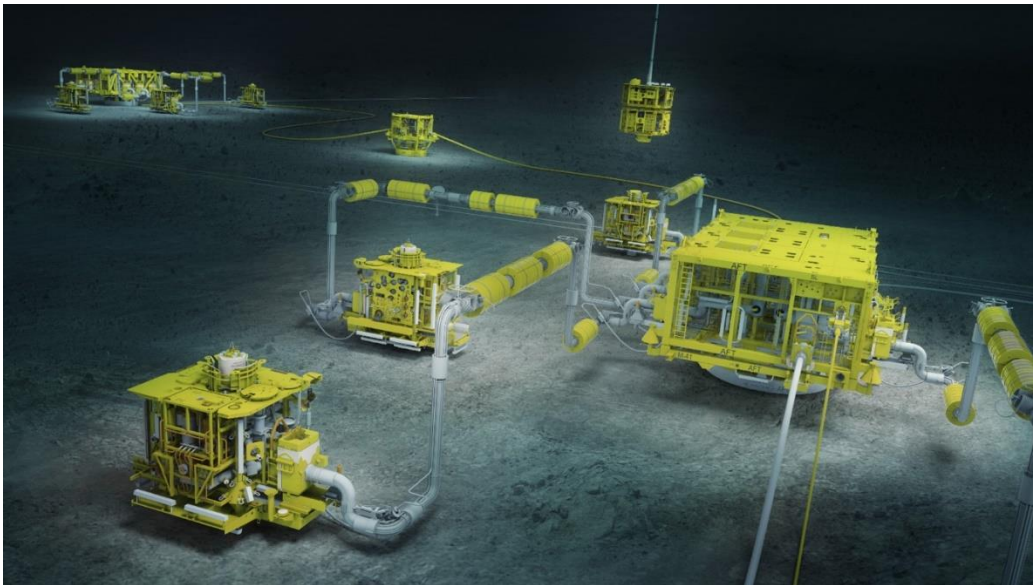
Figure 2.2 Subsea production system concept **(AkerSolutions, 2018)**

2.1.2 Wind turbines

One of the most promising alternatives for producing green energy is wind turbines. Wind turbines can essentially be placed wherever there is a lot of wind regularly. This could be on both land and in the ocean. The first offshore wind project was installed off the coast of Denmark back in 1991 (Bureau of Ocean Energy Management, 2016). Offshore wind farms operate in shallow waters around the world.

There are several advantages to placing wind farms offshore. As the ocean is a big open area, the wind speed tends to be steadier than on land. The wind speeds are often faster than on land as well, faster and reliable wind means a more reliable source of energy (American Geosciences Institute, 2018). Although there are some great benefits with offshore wind energy, there are also some drawbacks. The most noticeable being the cost of installing and maintaining offshore wind farms. The robustness is also an essential factor when regarding offshore wind farm. Being placed in the ocean these wind turbines are regularly exposed to waves, high winds and corrosion. One of the goals when installing offshore wind farms is that they are able to last 25 years and cheap enough to be able to replace as much fossil fuel as possible from coal, oil and gas (Midling, 2015).

Figure 2.3 Illustration of offshore wind farm **(Nelson, 2017)**

2.2 Numerical methods

2.2.1 Wave load mathematics

It is essential to have some knowledge on the math involved to understand the effect of wave loads on coastal structures. By simple hand calculations, it is possible to establish a solid baseline for the forces working on an offshore coastal structure. Waves hitting the cylindrical structure can be defined by some simple equations.

$$A = \frac{H}{2}$$ 2.1

$$T = \frac{2\pi}{\omega}$$ 2.2

$$L = \frac{2\pi}{k}$$ 2.3

$$v = \frac{\omega}{k}$$ 2.4

Equation 2.1, 2.2, 2.3 and 2.4 show the wave amplitude A, wave period T, wavelength L and wave velocity v, respectively. H is the wave height in meters, ω is the angular frequency and k is the wave number. Wavelength can also be indicated by using λ instead of L. It is possible to write the expression for a simple harmonic wave function as:

$$y = A \cdot \cos(kx \pm \omega t)$$ 2.5

Equation 2.5 has taken into consideration both positive and negative direction for X-direction (Physicskey, 2017).

To find the force acting on a structure, Morison equation is used. Morison equation calculates the force applied to a body. For a fixed body in oscillatory flow, the equation can be derived as:

$$F = \rho C_m V \dot{u} + \frac{1}{2} \rho C_d A u |u|$$ 2.6

The Morison equation 2.6 is a combination of both inertia and drag force.

The inertia force:

$$F1 = \rho C_m V \dot{u}$$ 2.7

Equation 2.7 is the sum of the Froude-Krylov force. Where $\dot{u}$ is the flow acceleration. V is the volume of the body, ρ the fluid density and C_m is the inertia coefficient. The inertia coefficient C_m is the same as $1 + C_a$ which equals the added mass coefficient.

Drag force:

$$F_D = \frac{1}{2}\rho C_d A u |u|$$

2.8

The flow velocity $u|u|$, is written like this to ensure that the drag force is always in the direction of the velocity. A simplification would be to use u^2. A is the reference area and C_d the drag coefficient. By using both the inertia force and drag force it is possible to get a good indication on how the wave loads affect the coastal structures.

2.2.2 Finite Element Method

There are several tools available to model and analyze any given physical phenomenon. One of these is the finite element method. FEM is a method to define a numerical approximation of the problem, which can be solved with a computer. FEM is used in a finite element analysis to investigate or asses the strength of a structure. The elastic behavior of a solid can be mathematically described in form of Partial Differential Equations (PDE). This is done by combining the kinematic equation and the material law into a momentum equilibrium equation (Piehl, 2017). The momentum equation can not be solved directly for complex geometries, this is why a numerical method like finite element method is used.

"In a PDE, we always have a mathematical expression describing the relation between dependent and independent variables through multiplications and partials" (Singh). The PDE contains unknown multivariable functions and their partial derivatives. It is used to formulate problems involving functions of several variables. The equations based on PDE contains partially derivatives, such as the wave equation:

$$\frac{\partial u}{\partial t} = \frac{\partial^2 u}{\partial x^2}$$

2.9

The variables x and t are independent of each other, and u is regarded as a function of these. Two other common partial differential equations are the Poisson 2.10 and Laplace 2.11 equations:

$$\Delta\varphi = \frac{\partial^2 u}{\partial x^2} + \frac{\partial^2 u}{\partial y^2} = f$$

2.10

$$\nabla^2\varphi = f$$

2.11

From equations 2.10 and 2.11 the $\Delta = \nabla^2$ is the Laplace operator and φ is a scalar function (Lindqvist, 2005, s. 2).

2.2 Numerical methods

While there is much mathematics behind a FEM, there also has to be a model of the object in focus. This could be a 3D model of any given object with the desired geometry. With a 3D model ready, it is possible to apply boundary conditions. Boundary conditions are restrictions set on the model to get a realistic comparison to a real-life situation. Some examples of boundary conditions are material, directional constraints, symmetry if there are any simplifications and applied force to the model. Directional constraints could be to fix all translational movement and only let the rotational degrees of freedom be free.

How accurate the result from a FEM is will depend on the boundary conditions, but also the mesh applied to the object. A mesh is a grid of small cells applied to the whole structure. How dense these cells are, and how well they interact with each other will affect the result. A coarser mesh will run the simulation faster but give a more inaccurate result. A finer mesh takes longer to compute but gives a more accurate result. There are also ways of getting a faster computational time with an accurate result. This could be done by splitting up the model in sections and then applying a coarser mesh on the parts of less importance and a finer mesh on the important parts. Symmetry is also a way of reducing computational time.

With the boundary conditions applied, the simulations can be run. There are various results from a FEM, what to look for will depend on the reason for using FEM. Some of the results could be stress on a specific area or displacement.

Figure 2.4 Simple FEM procedure illustration **(Prokos, 2019)**

Figure 2.4 shows a simple FEM procedure. First, a 3D model is made, mesh applied, boundary conditions are set, and the simulation is run with the result showing to the right.

2.2.3 Computational Fluid Dynamics

When working with fluids it is crucial to know how the fluid behaves. This could be the general fluid flow or how the fluid interacts with an object. A tool that is used to analyze a fluid flow is computational fluid dynamics. CFD is a numerical tool to solve or approximate the Navier-Stokes equation. In a CFD analysis, the examination of fluid flow is kept in accordance with its physical properties such as velocity, pressure, temperature, density and viscosity (SimWiki, 2018). It is also possible to simulate for multiphase flows.

To describe the motion of viscous fluid substances, the Navier-Stokes equation is used. The Navier-Stokes equation is defined by two coupled equations: the continuity equation 2.12 and the conservation of momentum 2.13 (Kundu, Cohen, & Dowling, 2012).

$$\nabla \cdot \boldsymbol{u} = 0 \qquad\qquad 2.12$$

$$\frac{\partial u}{\partial t} + (\nabla \cdot \boldsymbol{u})\boldsymbol{u} = -\frac{1}{\rho}\nabla p + v\Delta \boldsymbol{u} + \frac{1}{\rho}\boldsymbol{f} \qquad\qquad 2.13$$

Equations 2.12 and 2.13 state the incompressible unsteady Navier-Stokes equations in their differential form. In the equations u is the velocity vector, scalar pressure p and volume force is f (e.g. gravitation). The fluid properties are defined by the kinematic viscosity v and the density ρ. In the conservation of momentum equation 2.13, the left side is the product of fluid density times the acceleration that particles in the flow are experiencing. The right side has forces that are responsible for particle acceleration (Iska, 2017).

A common discretization technique used in CFD is the Finite Volume Method (FVM). "The FVM is a numerical method used for partial differential equations that calculates the values of the conserved variables averaged across the volume" (Weisstein, 2018). Similar to the finite element method, values can be calculated at discrete places on a meshed geometry.

When solving problems that include waves a two-phase solver is needed. This means that there will be a free water surface to solve. A common approach to numerically model the free surface is the Volume of Fluids method (VOF). "The volume of fluids method is an efficient technique for numerically treating free boundaries embedded in a calculational mesh of Eulerian or Arbitrary Lagrangian-Eulerian cells" (Nichols & Hirt, 1981).

The flow around a smooth cylindrical object can be described with the non-dimensional Reynolds number:

$$Re = \frac{Du}{\upsilon}$$

2.14

For equation 2.14 D is the diameter of the cylinder, u is the flow velocity and υ is the kinematic viscosity. How high the Reynolds number is will give an indication of how the flow behaves. The flow is often split into laminar and turbulent flow. The transition between laminar and turbulent flow often starts at about 2300.

Reynolds number can also be used when looking at the wake flow that is left behind the cylinder. The wake flow in a steady current starts to change to turbulent when 200 < Re < 300 as shown in Figure 2.5. When reaching Re=400, the vortices, once formed, are turbulent (Fredsøe, 2006).

	Laminar vortex street	40 < Re < 200
	Transition to turbulence in the wake	200 < Re < 300

Figure 2.5 Flow around a smooth, circular cylinder in a steady current **(Fredsøe, 2006)**

2.2.4 Examples

With the previously explained methods, it is possible to get various information about the case being investigated. For both the FEM and CFD method, the results are visualized in models that display specified information. This visual model shows a numerical value of information along with an indication of where on the object this is related to.

For the finite element method, the interest is often related to structural behavior. With boundary conditions applied to replicate realistic conditions is it possible to analyze both displacement and stress on the object, amongst other results.
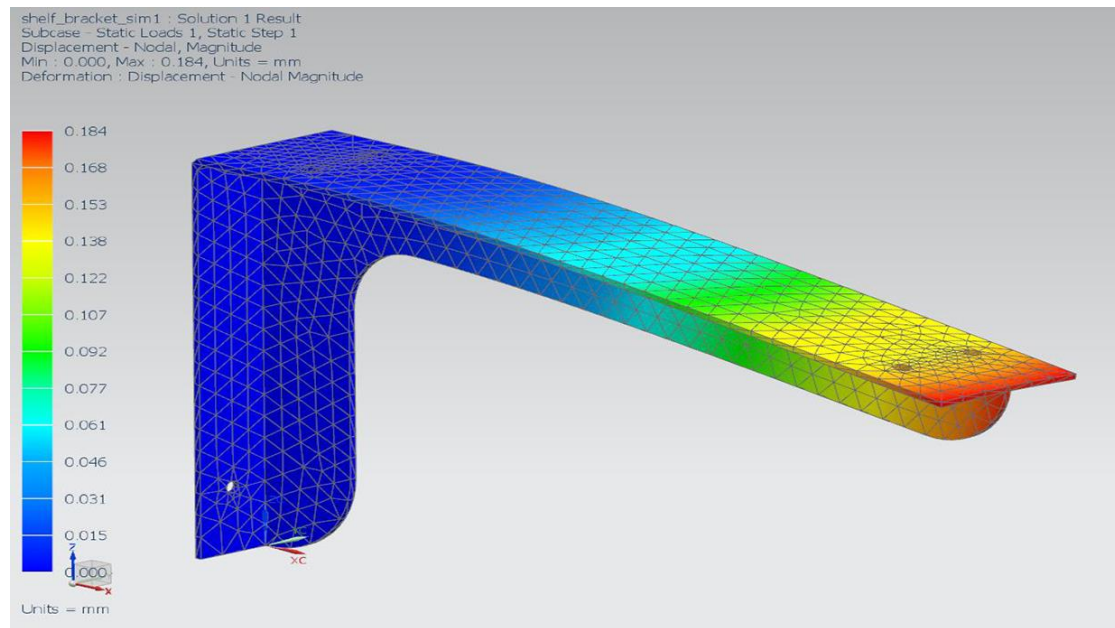
Figure 2.6 FEM bracket result example **(Skogsfjord, 2014)**

Figure 2.6 shows a simple bracket that has been used in FEM analysis. From the color indication along with the scale at the left side, it is possible to see that the maximum displacement is 0.184 mm. The stress is not shown in this picture, this is shown separately. From the blue color indication at the left on the bracket, it can be assumed that it has a fixed constraint there. The force has been applied on the tip where the color turns toward red, indicating the point with the most displacement. With this analysis, it is possible to determine if the results with the given geometry are satisfactory.

Computational fluid dynamics also provide a visual representation of the results. To get the most accurate results from a CFD analysis it is important to let the simulation run long enough so the fluid flow can stabilize. A program used to run CFD simulations is STAR-CCM+.
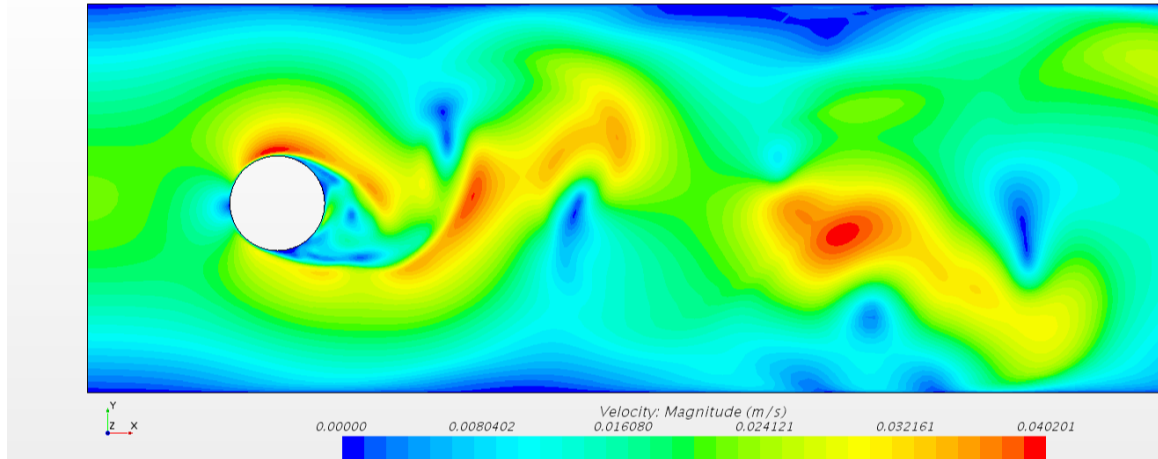
Figure 2.7 CFD fluid flow example

To illustrate how a CFD result could look like, the flow around a cylindrical structure is shown in Figure 2.7. This is a simulation of laminar flow with Re=1000. From the color indication, it is shown that the velocity varies, with the highest value of 0.04 m/s.
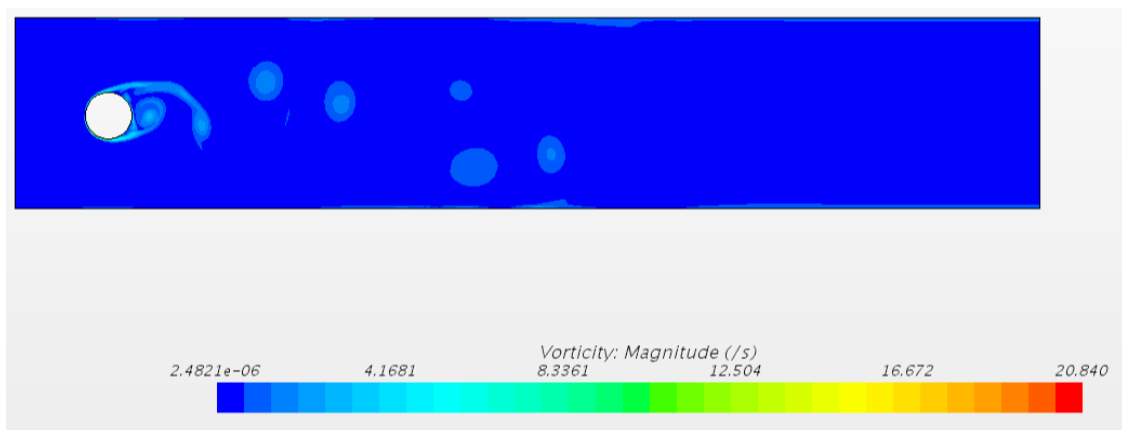
Figure 2.8 Vorticity example in CFD

Figure 2.8 shows the vorticity as a result of the fluid flow in Figure 2.7. The vorticity describes the revolving motion of a continuum near a point, in this case the cylindrical structure. This vorticity occurs when the flow is not hitting the cylinder straight on, but rather have an offset from the center.

2.3   Experimental methods

2.3.1 Model scale test
Model scale testing is an efficient way of determining how an object will behave in a real-life scenario. A model scale test is based upon taking the intended size of an object and scaling it either up or down. The most common way is to scale down an object. The scaled object is then modeled and tested in a controlled environment. These tests have a wide range of variety.

There are several benefits to using model scale tests. The most obvious being to reduce cost. Testing a scaled version of the intended size can save a lot of money and time. It also helps to validate the design and various aspects of the intended full-scale object. Model scale testing is used for numerous experiments. One area where model scale testing is frequently used is for designing a ship hull. "Traditional ship model tests provide still more accurate predictions of ship performance than existing computational fluid dynamics (CFD) methods can deliver" (Wärtsilä, 2018). By performing a scaled model test for ship hull, it is possible to evaluate ship resistance, propulsion and maneuvering. With the inaccuracy a CFD simulation may carry, a scaled model test could help validate the results.

When using a scaled model, it is important that the scaling is done correctly. It is also important to get the details as close to full-scale as possible. The physical properties may also affect the test results. Changing the scaled model is more efficient than making changes to a full-scale model. This is why a scaled model is often used in the design phase.

2.3.2 Wind turbine examples
A standard practice in the design process for offshore floating structures is model basin testing. This is also the case for floating offshore wind turbines. The DeepCwind Consortium at Maritime Research Institute Netherlands (MARIN) has done research for a 1/50th scale model test on various platform types. "The research was able to capture the global dynamic behavior of commercial scale model floating wind turbine systems. However, a mismatch in Reynolds number between full scale and model scale was found. Resulting in the strictly Froude-scaled, geometrically similar wind turbine underperformed greatly" (Fowler, Kimball, Dale, & Goupee , 2013). The research had to be modified in order to match existing wind turbine aerodynamic loads, such as thrust. More accurate results could be achieved if the model wind turbine matched more closely to the performance of a full-scale design.

Another research on model-scale offshore wind turbine has been to replicate a 50-year wave condition. The model is a stiff cylinder mounted on a spring, allowing rotation of the system around the base only in the wave propagation direction (Suja-Thauvin, Krokstad, & Frimann-Dahl, 2016). From the experiments, it is found that the maximum responses are recorded when long steep breaking waves hit the cylinder. An essential part of the research is to include the right damping when assessing the maximum loads. No slamming model was required to match the experiments. The research however does not aim at replacing state of the art theoretical models for estimating maximum loads on offshore wind turbines (Suja-Thauvin, Krokstad, & Frimann-Dahl, 2016).

3 Methods

3.1 Design setup

Measuring the exerted force from waves hitting a cylindrical structure can be done in various ways. What method to choose will depend on the goal of the research and available time to conduct the research. For this thesis one of the goals is to develop a numerical test tank. The focus is mainly to get a working numerical model that can be used for later research. To ensure the validity of the numerical model, an experimental test is conducted. With this comes additional limitations regarding available equipment.

3.1.1 Model dimensions

One of the things that had to be decided early on was the size of the cylinder to be used in both numerical- and experimental testing. To give the thesis more relevance to a real-life situation, the dimensions are roughly scaled after the wind turbine in Figure 3.1. The figure is based on a 5-MW offshore wind turbine with a monopile foundation. With this information, it is possible to find the height to width ratio and use this to determine the diameter to use for the numerical- and experimental testing.
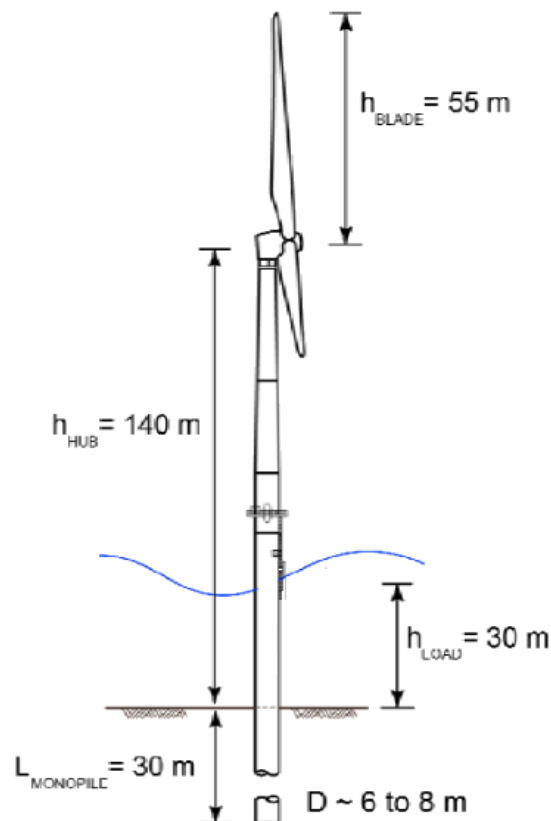

Figure 3.1 Wind turbine dimensions used as reference **(Cuellar, 2012)**

3.1 Design setup

In Table 3.1 the scaling factor between height/width is used to find the new diameter *d* that is used for the numerical- and experimental models. Setting the model height to 1 m is a simplification of the model to make sure that it is possible to use the cylinder in the wave tank. The diameter is rounded up to 60 mm for practical reasons. Both the numerical model and the experimental tests use these dimensions. With the height simplification, the test setup has a scale of 1:140.

Table 3.1 Model scaling

Scaling factor δ		17,5
	Full scale [m]	Model [m]
Length *L*	140	1
Diameter *d*	8	0.057

Another limitation for the setup is the size of the available wave tank. Since the size of the wave tank is predetermined, the numerical setup has to be identical. Using the same parameters is important to reduce any potential sources of deviation. Table 3.2 shows the dimensions for the wave tank used in the experimental testing and the dimensions used for the numerical model. The total length of the tank is not included in the numerical model, this is to compensate for the dampening beach that takes up some space. The cylinder is placed in the same place for both the experimental- and numerical testing. This is at 4 m from the wave starting point allowing the waves to sufficiently develop before reaching the cylinder.

Table 3.2 Wave tank characteristics

	Actual tank	Numerical model
Length [m]	10.9	9
Width [m]	2	2
Water depth [m]	0.8	0.8

3.2   Experimental testing

When developing new models or procedures for research purposes, some sort of validation is beneficial to boost credibility. One way of verifying the numerical results for this thesis is by doing scaled experimental testing in the wave tank available at the university. With the wave tank, it is possible to generate waves with various parameters up to a certain limit and use a load cell to register the exerted wave force. It is important to note that the wave tank available has some limitations regarding size that could affect the results.

To make the research more efficient and save time with the numerical models, it was necessary to establish the limitations by the tank early on. One of the most relevant data that is gathered from the experimental testing in the wave tank is the exerted force on an object from the waves. By determining what can be expected from the wave tank it is possible to get an indication of what magnitude to expect from the results on similar tests. This is a helpful method to find any deviations that should be investigated further.

3.2.1 Reference test

It was decided early on that a reference test was needed as a way of determining what forces could be expected from the waves in the tank. The goal was to set up a simple test rig with the available equipment in the wave tank. As an addition to the wave generator in the towing tank, there is a mobile trolley with a load cell attached. This load cell can be used to measure the exerted force from a wave hitting the cylinder. The load cell on the trolley operates on 4 Degrees of Freedom (DOF), missing left/right- and yaw movement. When registering the force on the cylinder it is the horizontal movement, back and forward that is of interest. The three other motions have to be locked so that the result is not affected. Figure 3.2 shows the load cell that is mounted to the trolley in the wave tank. It is also indicated where an external object is to be mounted with the number 1.
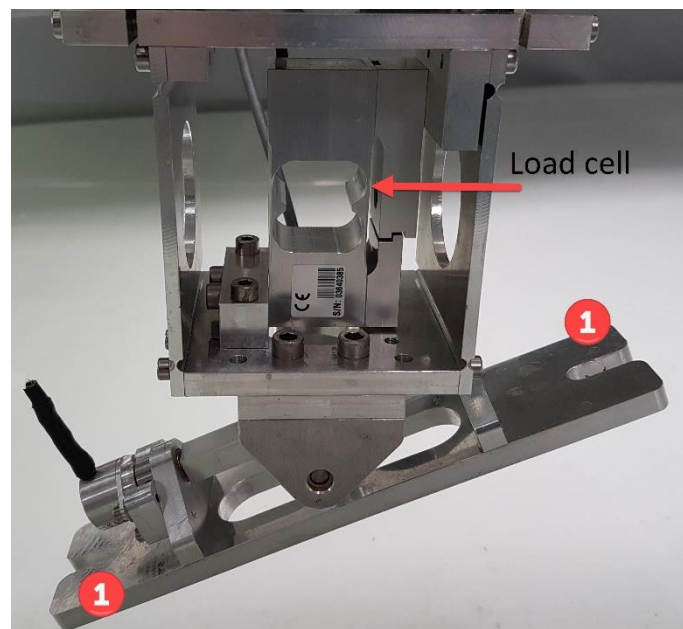

Figure 3.2 Load cell setup used for reference test

Another aspect that has an impact on the result, is not calibrating the load cell before use. Without calibrating the load cell, the user runs a risk of getting inaccurate data rendering the tests useless. The goal of the calibration is to get the load cell to read 0 when no external load is applied. This is done by applying a known load in the direction of the force in focus. With the load known it is possible to calculate what the force sensor should read. The sensors give data in [N], so if the load is 1 kg the sensor should read 9.81 N. If the sensor has some deviation from this the "gain" is adjusted to correct the data output. To further increase the sensor accuracy, more weight is added. With the "gain" adjusted all weights are removed, and the sensor should read 0. The sensor is then calibrated and ready for use.
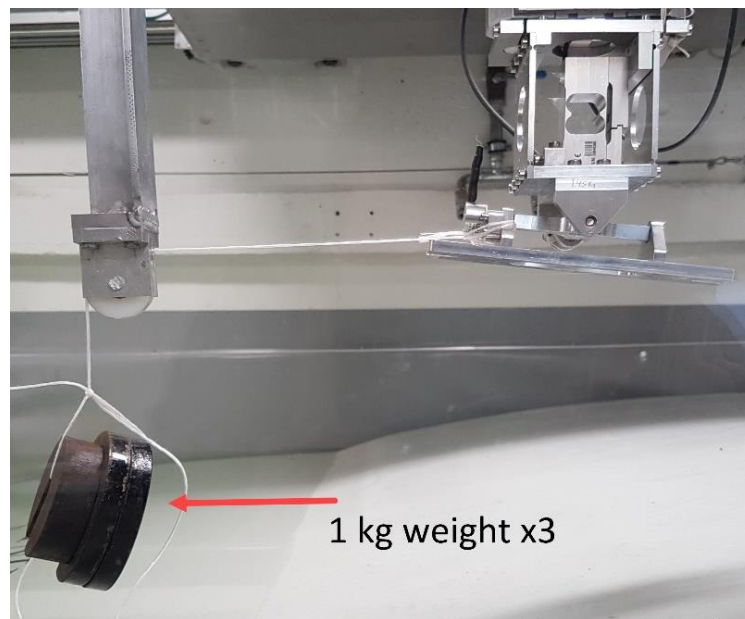

Figure 3.3 Calibrating the load cell with known loads

Figure 3.3 shows how the load cell can be calibrated by applying known loads. The force is applied horizontally by using a pulley that is attached to a simple beam. Each of the weights, at 1 kg each, are applied one at a time. The "gain" is adjusted for each new weight, making sure that the data output is corresponding to the weight. To get the most reliable results on the horizontal force, it is important to keep the mounting bracket under the loading cell as leveled as possible.

With the load cell calibrated, it is possible to get data from the generated waves by adding a cylindrical structure that goes down into the water. One aspect with the reference tests was to keep the design simple and easily adjustable. Figure 3.4 shows the model used for the reference tests. It is a simple design where a 50 mm plastic pipe is held in place by two pieces of wood. The pipe is held in place by screws on either side, making it easily replaceable. The first model was a hollow pipe but was later changed to a filled pipe. The hollow model tended to roll to either side, due to buoyancy. Simply sealing the hollow pipe also proved insufficient. With a filled pipe, this was no longer a problem. To prevent interference on the output data, three of the four degrees of freedom was locked. Only leaving forward/backward open. The number 2 in Figure 3.4 indicates where wedges are inserted to lock out roll and pitch movement.
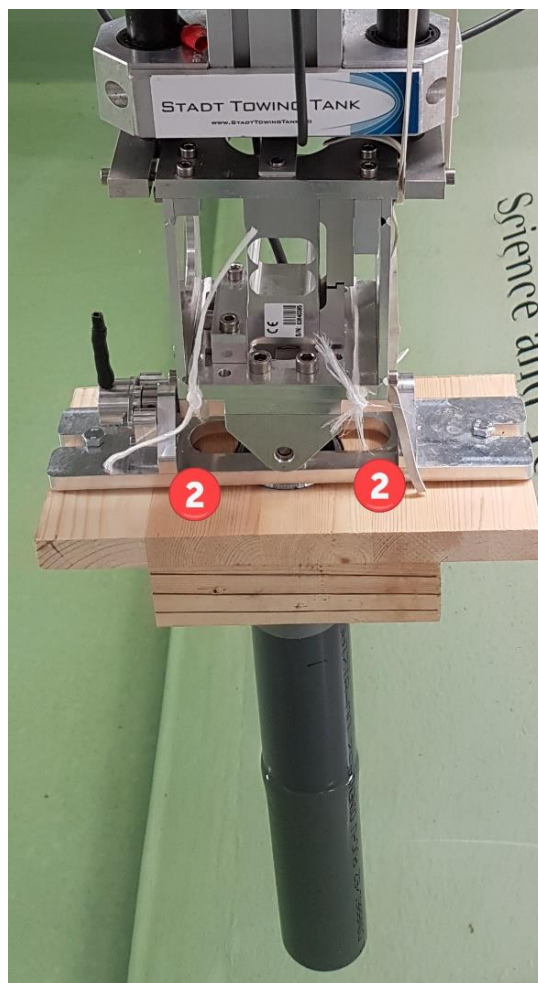

Figure 3.4 Reference test model

3.2.2 Scaled model testing

With the dimensions determined and the data from the reference test analyzed, it was possible to design a setup to use in the scaled model testing. One of the details that were decided early on was to use aluminum instead of steel. This was mostly due to the rigid structure of steel compared to aluminum. Since aluminum has a lower Young's modulus it will deform more easily, giving better results on the testing. Using steel could potentially lead to the structure being too rigid and not be affected by the waves.

The idea of the model testing was to simply weld a cylindrical pipe to a base plate. However, due to the fact that the generated waves from the reference test were showing a weak output, the design was altered. Instead of having the cylindrical pipe welded directly to the base plate, it was attached with a mounting bracket. Figure 3.5 and Figure 3.6 shows how the mounting of the cylinder is intended. This was done to make the setup more versatile in allowing for an easy way of changing the cylinder if needed. Originally three different cylinders were intended, each with different diameter. However, due to a lack of material regarding 70 mm aluminum cylinders, only a 50 mm and 60 mm cylinder was used. The setup is also more exposed to the force from the waves. With the less rigid structure at the base plate, it should be possible to register a higher force from the waves. The details regarding measurements on the design setup can be seen in Appendix D.

Figure 3.5 Base plate with mounting bracket

Figure 3.6 60 mm Cylinder

3.2 Experimental testing

To register data from the waves hitting the cylinder, strain gauges from HBM was used. Strain gauges were used for their high sensitivity and the possibility of choosing exactly where to place them on an object. The high sensitivity of the strain gauges is beneficial to the testing when doing tests that could potentially have a low force output as the case is with the wave tank. The strain gauges are also an inexpensive solution that provides high accuracy. The manufacturer provides a Gauge Factor (GF) of 2,09 and resistance of 120 Ω. GF is the ratio of fractional change in electrical resistance to the fractional change in length or strain, as seen in equation 3.1 (National Instruments Corporation, 1998).

$$GF = \frac{\Delta R/R}{\Delta L/L} = \frac{\Delta R/R}{\varepsilon} \qquad\qquad 3.1$$

Installing strain gauges requires precision and careful handling. As a side effect of the high sensitivity strain gauges provides, they are easily affected by contamination. A single fingerprint leaving oil from the skin on the strain gauge can affect the data output. It is therefore important to keep the installation process as sterile as possible. Using gloves and a pair of tweezers could help reduce contamination. The tweezers also make for easier placement of the strain gauge as it is quite small. Figure 3.7 shows the size of the strain gauges that are used. It is also possible to see the direction of the wires in the strain gauge. The positioning of a strain gauge has to be so that the gauge wires are in the same direction as the stress to be measured. A strain gauge can only measure data in one direction.

In addition to keeping the installation process sterile, it is necessary to prepare the surface of the object. The first step is to sand down the surface where the strain gauge is placed with fine sandpaper. The sanding can be done in several steps, going up to 400 grit for the finest sanding. Sanding down the surface leaves fine scratch marks that will allow the glue to stick better. Loctite 496 is an example of an adhesive that can be used. After the surface has been sanded it is important to remove any residue that is left behind. This is done by wiping off the worst with some paper towel and water. When the paper looks clean, a lint-free gauss dipped in alcohol is used to remove any last residue and sterilize the surface.
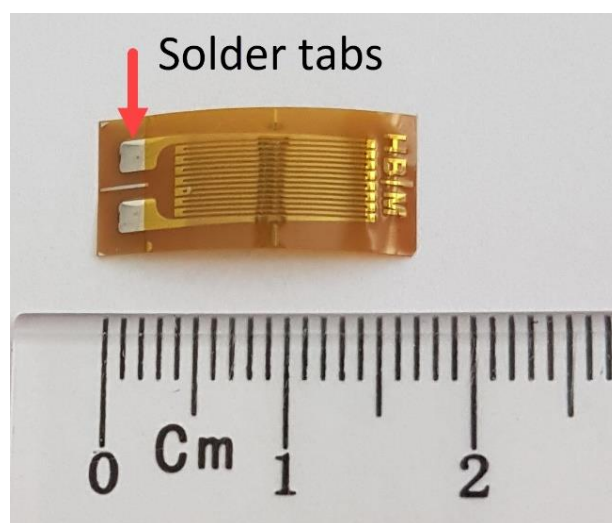

Figure 3.7 Strain gauge used in the experimental test

Before applying glue to the strain gauge and placing it on the mounting bracket, it is held in place by cellophane tape. Figure 3.8 shows how tape is used to hold the strain gauge. Placing the strain gauge with tape ensures that the positioning is correct by allowing for replacement if necessary. Only having tape on the top part of the strain gauge makes it possible to flip the strain gauge back and then applying glue on the sanded surface. A drop of glue is applied to the surface and spread out by using a piece of Teflon tape. With the glue spread out, the strain gauge is gently placed back down to the surface. The Teflon tape is then used to press down on the strain gauge while the glue sets. When the glue has hardened both the Teflon- and cellophane tape is gently removed. It is important to do this slowly and watch out for any indication of the strain gauge not being properly fastened. Strain gauges are installed on both sides of the mounting bracket using the same procedure.
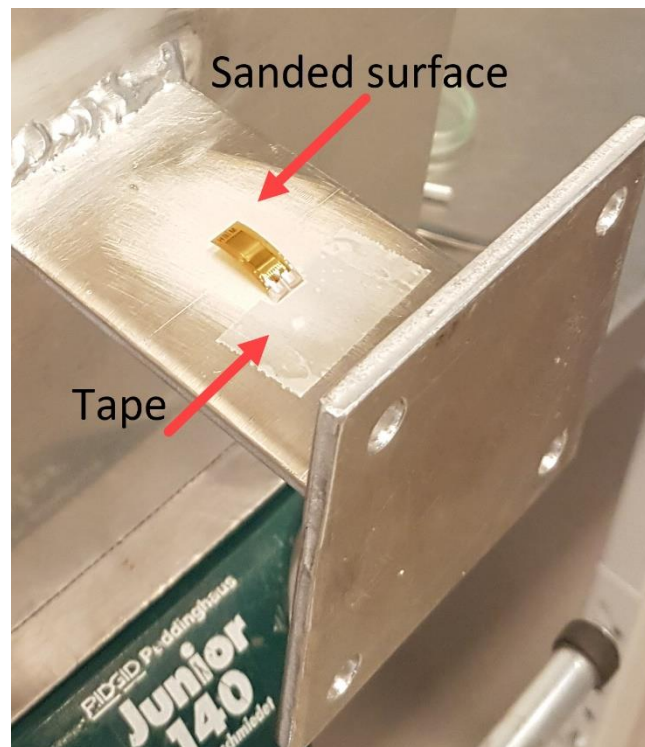

Figure 3.8 Placement of strain gauge

With the strain gauges properly installed, wires are soldered on. The strain gauges have solder pads integrated that are ready to use. Before wires are soldered on, the pads are sanded just enough to expose the copper. This way the wires have a better connection to the strain gauges. The strain gauges are also rinsed over with a lint-free gauss that has been dipped in alcohol to make sure the setup is still sterile. A good amount of wire is measured out before cutting it, making sure it is not too short. The wires are taped to the mounting bracket, going down to the base plate and out to one of the sides. This is done to keep the wires out of the way. The alternative was to run the wires up along the cylinder, but since this may cause interference on the wake behind the cylinder it was not done this way. It is also a more efficient solution since there is no need to attach the wires to the cylinder when setting up the test.

Since the strain gauges are placed under water, a layer of protective silicone coating is applied. The coating used is called "SG250" which is a transparent, single component silicone rubber (HBM, 2019). The coating is applied to a large area around the strain gauge to ensure that no water can come in contact. Figure 3.9 shows how the wires are taped and the silicone coating protecting the strain gauges. With the silicone coating hardened, the tape is replaced with a stronger tape more suited when in contact with in water.
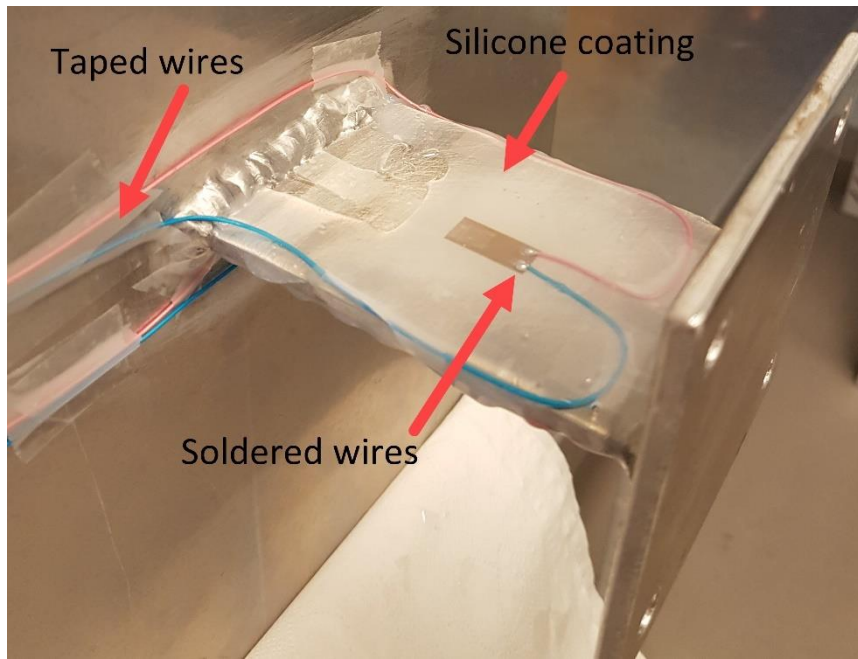

Figure 3.9 Strain gauges attached to the mounting bracket

With the strain gauges adequately attached and the wires soldered, the setup needs to be calibrated. This is done in the same fashion as with the reference test, using a known load and adjusting the data logger. Before applying a known load on the cylinder, it needs to be horizontally pointing. This is done by locking the base plate vertically in a vise, so the mounting bracket is pointing horizontally. Figure 3.8 shows a closeup of the base plate locked in a vise and the mounting bracket pointed horizontally. The cylinder is added, and a known load is inserted in the open end of the cylinder and the logging program is adjusted so the output is corresponding to the weight. The load used was a standard D battery, weighing 140 g. With the program adjusted and battery removed the output reads 0.

A part of setting up strain gauges is using a Wheatstone bridge. A Wheatstone bridge is an electric circuit used to measure minute changes in electrical resistance (OMEGA, 2019). The changes in electrical resistance are what the strain gauges use to measure the amount of force applied to produce stress on an object. A metal piece that is subjected to tensile stress will see an increase in length. As a result of this, the electrical resistance will increase. Similarly, if the metal is subjected to compressive stress, the length will decrease. This is also a change in electrical resistance (John, 2011).

3.2 Experimental testing

How a Wheatstone bridge circuit is configured will depend on the number of strain gauges used. The bridge can be set in three different ways such as quarter bridge, half bridge or full bridge. Quarter bridge uses one strain gauge, half bridge uses two strain gauges and full bridge uses four. For the cylinder both tensile stress and compression stress will be present, resulting in two strain gauges with a half bridge configuration. Figure 3.10 shows the half bridge setup used with the cylinder. With two strain gauges active, both compression stress and tension stress can be registered. When there is no strain applied to the cylinder, the output measurement will be zero. The Wheatstone bridge is then balanced. With stress applied, the bridge becomes unbalanced and produced an output voltage that is proportional to the input stress (John, 2011). Resistance is measured as a change in voltage, and this is what gives the force output from the stress applied. To get the correct output it is necessary to set the logger program to half bridge and not quarter- or full bridge.
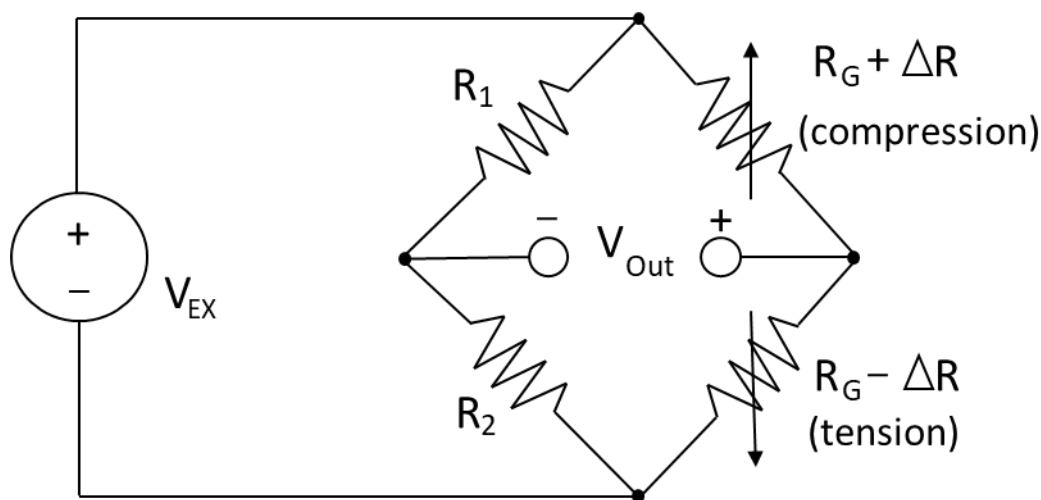

Figure 3.10 Half circuit Wheatstone bridge

When dealing with sensitive technology, there is also the possibility of background noise affecting the data output. Some of the sources that affected the registered data were the power outlet, electrical wave generator motor and the wires. To reduce the disturbance from the power outlet an isolated socket, away from other electronic devices, was used. The wave generator was not much that could be done with, but the effect from it disappeared when it was producing waves. The generator only gave disturbance when not producing waves. To minimize disturbance from the wires, they were twisted. Electrical wires have opposite magnetic fields of each other. Twisting them together makes the magnetic fields cancel each other out. This also cancels out any external magnetic fields. To further reduce any background noise, a grounding wire was added. These countermeasures resulted in the background interference being reduced to ± 0.05 Nm.

3.2 Experimental testing

To test the cylinder in various settings, several waves were generated with different parameters. In the wave generator, it is possible to set the type of wave, wave height and period. The waves used for the testing is set to regular waves not irregular. Table 3.3 shows the various parameters intended for each test.

Table 3.3 Setup configurations

Setup No	Set height [mm]	Actual height [mm]	Period [s]	Number of waves
1	100	70	1	5
2	150	40	2	5
3	200	50	2	5
4	200	50	2,5	5
5	250	70	2	5
6	250	40	3	5
7	300	70	2,5	5

An important note from the testing in the tank is the deviation from the set wave height to the actual wave height. As the table shows, the generated waves do not correspond to the set height. This is a consequence of the wave tank not being calibrated. After the initial tests, it was quickly noticed that the dampening beach at the end of the tank had little to no effect on the waves as the waves were not able to wash over the beach. To remedy this, the water level in the tank was raised so that the waves were able to wash over the beach and dampen out more efficiently. It is likely that raising the water level in the tank also had an effect on the tank calibrations and thereby wave height.

To measure the actual wave height a scale was added to the cylinder, and the results recorded. Figure 3.11 shows the cylinder with the added scale, where 0 represents the calm water level. The test parameters are taken from setup 1, which should give a wave height of 100 mm. The actual wave height only reaches 70 mm, as shown in the figure. A deviation like this is also the case for the remaining setups used in the testing.
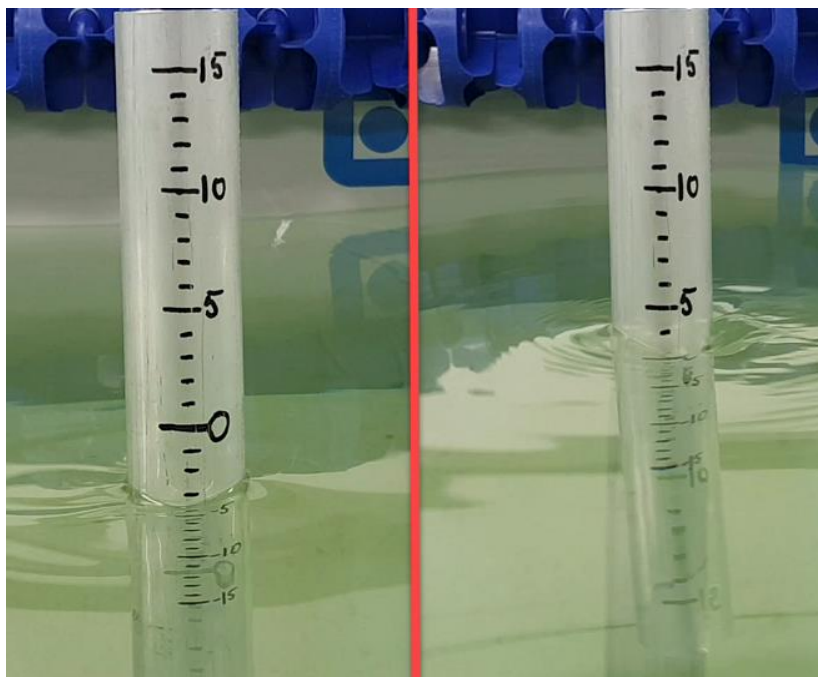

Figure 3.11 Screen capture from setup 1 with scaling [cm]

3.3   Numerical simulation

3.3.1 FEM model

When doing any testing, a good model can help the process. This is how FEM can be a helpful tool for the design process. With a virtually developed model, it is easy to make changes or test new designs efficiently. A 3D view of the model can help the user see things from different perspectives, giving a more detailed insight into the design. In some programs, simulations are used on the model to see how it will act if a force is applied. To design the test setup, Siemens NX was used. Siemens NX is a program where it is possible to change the details of the model by using expressions. This is a function that allows the user to make quick changes to the model and set certain parts to be dependent on each other. One such pairing of parts was to set the relation between inner and outer diameter to a fixed value. If the outer diameter is changed, the inner diameter automatically follows.

The first model done in NX was a simple hollow cylinder attached to a flat base plate. This model was used to investigate how an external force would affect the cylinder and to test out various dimensions. Since the forces from the generated waves are quite low, the setup was made so that the waves could have the biggest possible effect on the cylinder. One of the changes to the design was to adjust the wall thickness. The first tests had walls that made the setup too rigid, and thereby they yielded no usable results. With thinner walls and changing from steel to aluminum, the setup started to yield applicable data. Figure 3.12 shows the first intended design for the experimental test setup. This was the most straightforward and fastest solution, but not the most practical regarding changing cylinder or fastening strain gauges.
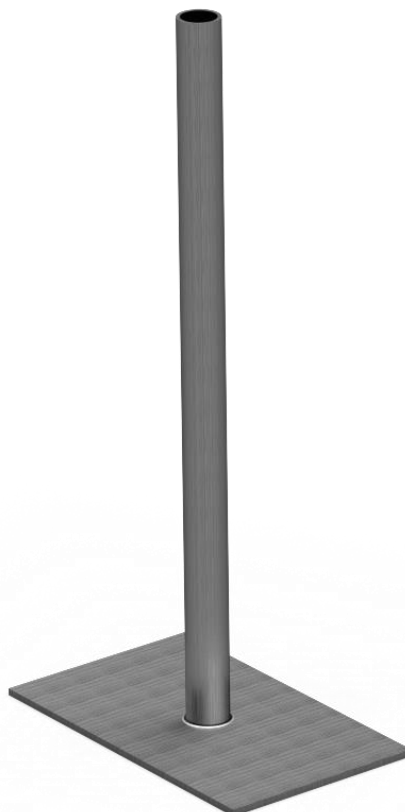

Figure 3.12 First virtually developed test design

3.3 Numerical simulation

Siemens NX was also used to make the machinery drawings that were the basis for producing the test rig to the experimental testing. This way of virtually developing a 3D model to work with before sending the specifications to production has been beneficial to the design process. With a 3D model, it is easier to see how a solution will fit with other components, or if it is even possible to produce the desired part. The base plate with the mounting bracket attached was designed this way. The mounting bracket was designed after how big the attachable cylinders were. For the experimental tests in the wave tank, two cylinders were used but the mounting bracket was designed to fit a 70 mm cylinder as well. To see if the parts fit together, an assembly was used. Here it is possible to import the needed parts and use constraints to assemble the parts.

Figure 3.13 Assembly of 60 mm cylinder attached to base plate

3.3 Numerical simulation

Setting up the geometry with desired dimensions is the first step of any FEM simulation. Figure 3.13 shows the finished assembly of the model with the correct dimensions. The dimensions used in the model corresponds to the dimensions used in experimental testing. Before simulating the model, certain configurations have to be made. This includes material selection, applying a mesh, force and constraints. As mentioned previously, aluminum is used due to a lower Young's modulus than steel. The applied mesh is a simple 3D tetrahedral mesh, a fixed constraint is added underneath the base plate and the force applied is in the same range as found in the reference tests. To simplify the setup the force is applied at the top of the cylinder, making the distance to the base plate 1 m.

3.3.2 Analytical method

As an addition to the numerical simulations, control calculation is done. This calculation looks at the displacement in the cylinder after a force is applied.

$$y = \frac{Fl^3}{3EI}$$
3.2

Equation 3.2 shows the formula used to calculate displacement. *F* is the force applied to an object at a distance *l* from where the object is fixed to a point. *E* is Young's modulus and *I* the moment of inertia. The applied force is of the same magnitude as the one found from the reference testing. Young's modulus is found in aluminum material properties from NX. Moment of inertia for a cylinder is derived from Equation 3.3, where *D* is the outer diameter and *d* the inner diameter of the cylinder. Equation 3.4 is the moment of inertia for a rectangular cross-section, where *H* is the height and *B* the width.

$$I_x = I_y = \frac{\pi}{64}(D^4 - d^4)$$
3.3

$$I_x = \frac{1}{12}BH^3$$
3.4

This way of controlling the numerical model does not take into consideration that the cylinder is attached to a mounting bracket. The formula in equation 3.2 is meant to be used on a straight object with one end free and the other fixed. The calculation is therefore done on the first test setup as seen in Figure 3.12. With this setup, it is possible to compare the results from the numerical model to the calculation from equation 3.2. By controlling that the results are relatively close, it can be justified that the numerical model has the correct setup. The actual model is then simulated with the correct configurations.

3.3.3 CFD

Computational fluid dynamics is a helpful tool when simulating flow around an object. By using CFD, the user can see how a fluid will behave when interacting with an object. For the cylinder placed in the tank, it is the exerted wave force that is of importance. Another aspect that is of interest is the flow around the cylinder. How to set up a CFD simulation depends on what is being investigated. There are several aspects that have to be taken into consideration for the various cases. How to model the geometry, setting up the mesh, solver configurations and boundary conditions are all examples of necessary parts in the setup procedure. To run a CFD simulation on the cylinder, Star-CCM+ is used. Setting up a CFD simulation can be a time demanding operation, it is also challenging to make changes once the setup is complete. In order to quickly change the case setup, Star-CCm+'s macro scripts were used to change parameters. A macro is a file that saves the changes the user makes up until a point where it is stopped. By splitting up the whole process into smaller steps it is possible to save time by not having to start fresh if there is something wrong with the model. If there is something wrong with the setup, the user can go back to a point where the model was working by loading the corresponding macro to that point.

Setting up the desired geometry is the first step in any CFD simulation. In addition to setting up a geometry model, the domain surrounding it is added. The cylinder and the domain surrounding it is modeled with the same parameters as the wave tank that is used for the experimental testing. The only deviation being the length of the tank. A shorter tank in the CFD simulation is a result of the dampening beach being excluded. This also helps save computational time on the simulation with fewer cells to solve. Another simplification on the CFD simulation is the available space for air. This is set to 0.2 m, making the total height of the domain 1 m. Limiting the domain as much as possible is beneficial to save computational time.
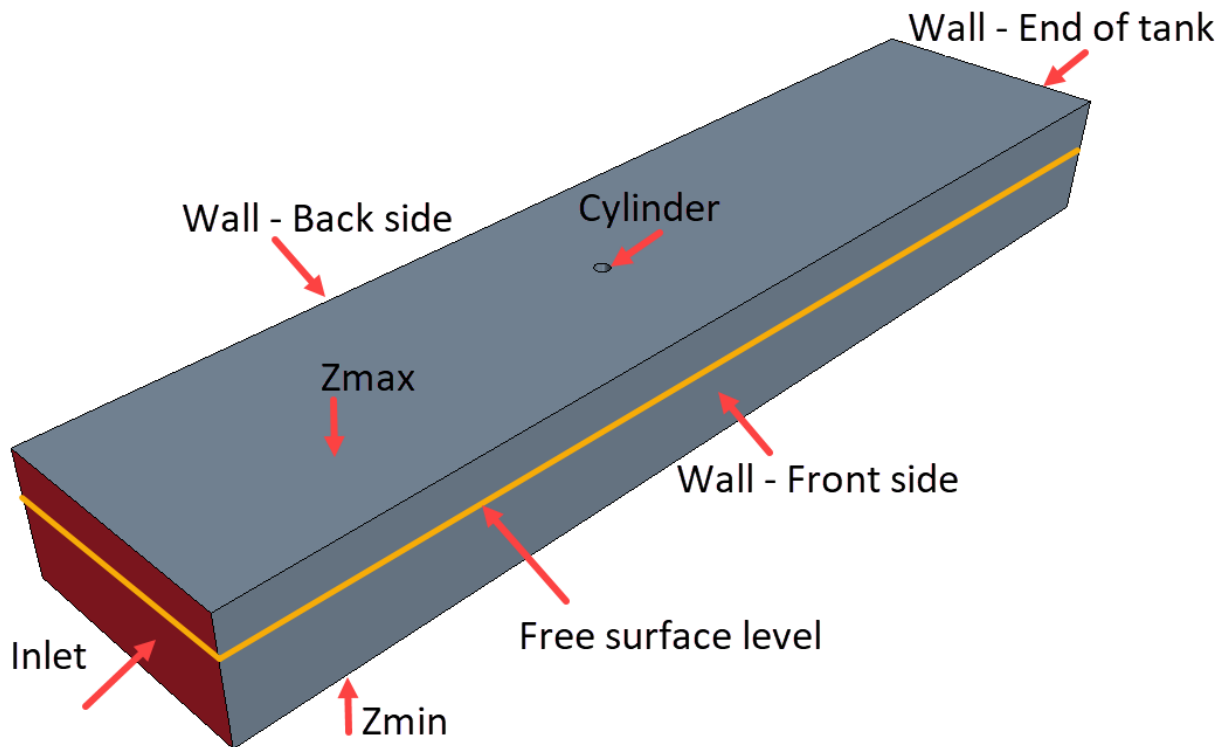

Figure 3.14 Model of domain around cylinder

3.3 Numerical simulation

Figure 3.14 shows the model used to do the CFD simulation. The domain surrounding the cylinder is scaled after the wave tank with the exclusion of the wave beach. Each of the surfaces is named and assigned to a specific purpose. Inlet is assigned to velocity inlet while the remaining surfaces are all assigned to a wall function. The free surface level is marked by the yellow line.

It is important to be aware of how the model is oriented. As a default setting, the height of VOF waves goes in Z-direction. The model is therefore oriented so that the waves move along X-direction, with Z-direction being wave height. Another default setting is the VOF waves starting where Z is 0. To get the waves starting at the right height, the model is sketched in the XY-plane. The domain is represented by a rectangle and the cylinder by a circle. With the placement correct, the sketch is extruded asymmetrically in Z-direction. One side is extruded 0.2 m to accommodate for air and the opposite side extruded 0.8 m for the water depth. This way of setting up the model ensures that the coordinate system is placed where the extrude starts, and thereby the waves start where Z is 0.

With the geometry in place, a mesh is applied. A good mesh is needed for the simulation to yield accurate results. When setting up a mesh there are several aspects that have to be taken into consideration. The first thing that has to be determined is where there is a point of interest. For the wave tank, it is the cylinder that is in focus. It is also of interest to see how the waves develop and how they act on the cylinder. On these areas of interest, the meshing is finer with more cells used. This is referred to as a refinement zone. A refinement zone is gradually scaled down from the bigger base mesh, providing a smooth transition to the smaller cells. Using more cells gives a more accurate result, but also increases computational time. To save computational time, refinement zones are only used where necessary while the rest of the domain has a coarser mesh.
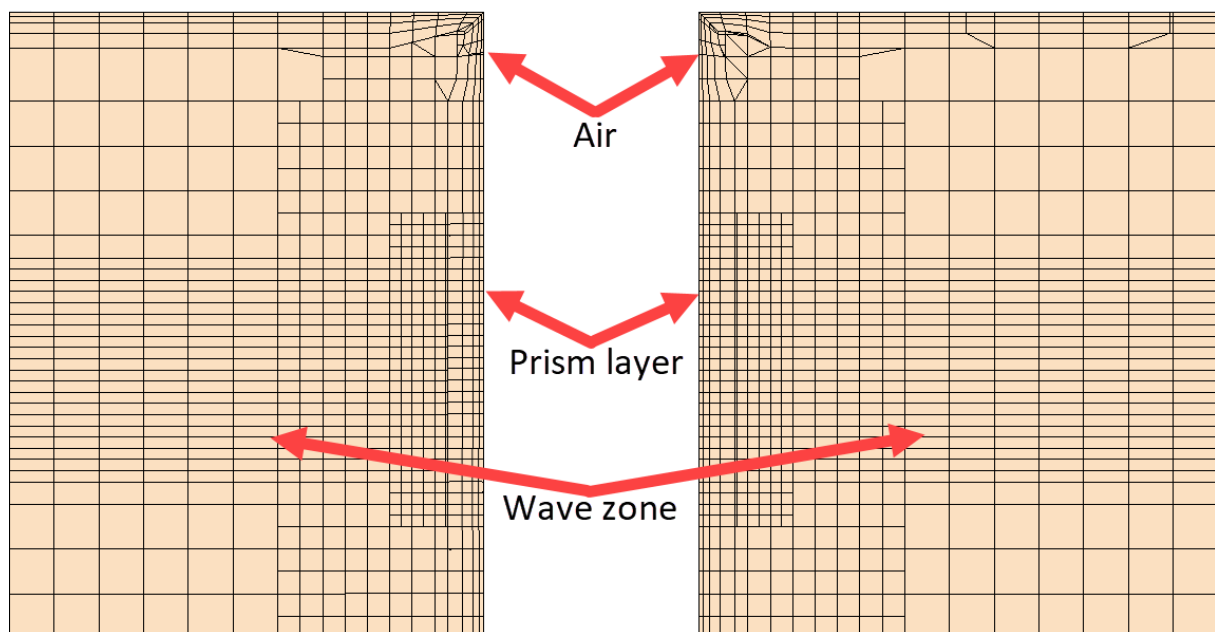

Figure 3.15 Plane section view of mesh around cylinder

3.3 Numerical simulation

In Figure 3.15 the close-up mesh around the cylinder is shown. The figure shows how the cell size varies, depending on what is in focus. At the top of the cylinder, where there is air, the meshing is coarse and not so neatly aligned. This done to save computational time as this is not an area of interest. The areas with better cell alignment and more cells start under the layer of air, where the waves interact with the cylinder. In this transition zone, a prism layer is added around the cylinder. The prism layer consists of several small cells and is needed to solve the waves moving around the cylinder. Having too big cells around the cylinder would give inaccurate results as there is less data to base it on. To see how the waves develop a mesh refinement is applied along the free surface, following the water level. The mesh is fine enough to account for all the simulated waves. Cell generation is done differently for the wave zone. Instead of having isotropic cells as the rest of the mesh, anisotropic cells are used for the wave zone. The anisotropic cells are stretched out along the domain to improve computational efficiency and increase accuracy. The goal is to see how the waves develop along with the domain, by having longer cells along with the domain it is possible to fit more cells per wave height. One wave height should have between 10-20 cells. The cells should also have an aspect ratio of 4 for not so steep waves, as is the case for the simulations (Kalaskar, 2018). The aspect ratio is the length of the cell divided by height, which is set to 0.04 m and 0.01 m respectively.

With the meshing applied, solver configurations have to be made. Some of the most relevant models that have been chosen for the cylinder are implicit unsteady, Eulerian multiphase, volume of fluid, laminar flow and VOF waves. Implicit unsteady is an approach used for obtaining numerical solutions, for time-dependent PDE's. The method calculates a solution both for the current state of the system and the later one. A large local time step is also possible as the solver remains stable over a big range. The residuals also converge at a relatively good pace (Field, 2017).

Having a multiphase model is necessary when there is more than one fluid involved. For the cylinder simulation, both water and air are present. It is therefore necessary to set up models for each of the fluids, both with constant density. Volume of fluid is a free-surface modeling technique used to analyze the fluid flow. The flow around the cylinder is set to laminar since the waves are quite small. These small waves are part of the VOF waves. When using VOF waves, there are several different types. The most suited type for the cylinder simulation is first order VOF waves. These are similar to a sine wave.

3.3 Numerical simulation

An iso-surface is used to project the waves visually. The iso-surface is placed horizontally in the tank going along the length of the domain. From Figure 3.16, it is possible to see how the waves form and how they dissipate after time. As the waves are quite small, they are already dampening out before reaching the cylinder.
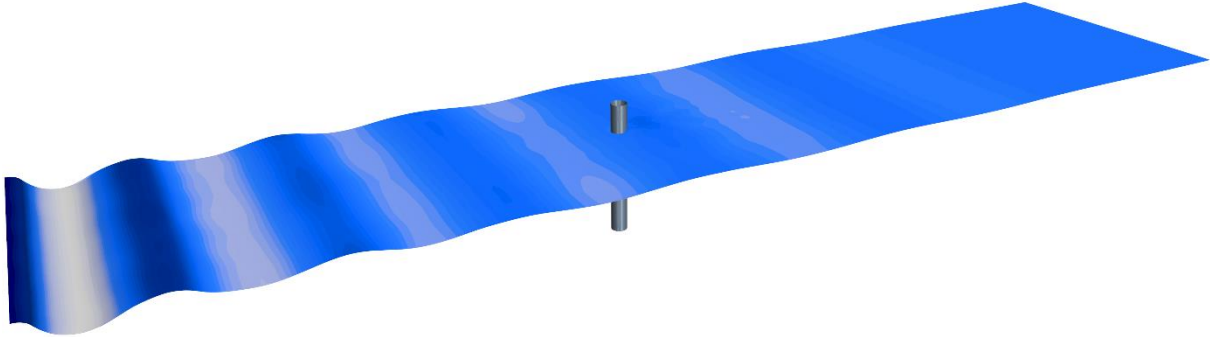

Figure 3.16 Iso-surface added to visualize wave development, setup 7

How smooth and fast the simulation will run is dependent on the solver settings. Using a fine mesh will have a significant impact on simulation time. As there are more cells to solve for, the computational time increases but so does the accuracy. It is therefore necessary to find a compromise that works with both simulation time and accuracy. Adjusting the timestep and inner iterations will also have an impact on the simulation results. Setting a low timestep results in the simulation taking too long, while a big timestep gives a rough result. The timestep is connected to inner iterations. By increasing the number of inner iterations, the results become more accurate and give the simulation more time to converge. This also comes down to a compromise, as more inner iterations also increase computational time. For the simulations, the inner iterations are set to 20, while the timestep is adjusted throughout the simulation. By starting the simulation with a high timestep, such as 0.1 s, the initial wave generation is expedited. Shortly after, when waves are starting to form, the timestep is reduced to 0.03 s. The results are plotted in a graph by adding a force plot on the cylinder.

To save simulation time, a smaller model was made to check all the configurations. This model was a smaller version of the wave zone without a cylinder. All the same solver configurations were added and tested. With satisfactory results that provided the correct waves, this was transferred to the full-scale model.

4 Results and discussion

4.1 Tests in wave tank

4.1.1 Results from reference test

The primary purpose of the reference test was to get an indication of what force magnitude to expect from the wave tank. It is important to note that the reference test was done with a 50 mm cylinder and not 60 mm as intended to use on the later testing. Another deviation from the actual tests is the length of the cylinder used. In the reference tests, the cylindrical plastic pipe is 22.5 cm long with only a portion of it in the water. The reference tests were done prior to the water level being raised.

To get a reasonable basis of what magnitude can be expected from the wave tank, the reference testing was done with a wide array of parameters. By changing the wave height and period, it was possible to do multiple tests with different results. It was also tried to use more than five waves per test but due to an error with the wave generator, this was not possible. Whenever more than five waves were generated, the machine stopped abruptly. This limited the wave generator and the testing capabilities. Figure 4.1 shows the first data collected from the reference test. The test is done with the same parameters as setup 1 from Table 3.3. Markings on the X-axis have been removed from the reference test as it is force magnitude that is the most relevant result for the reference test.
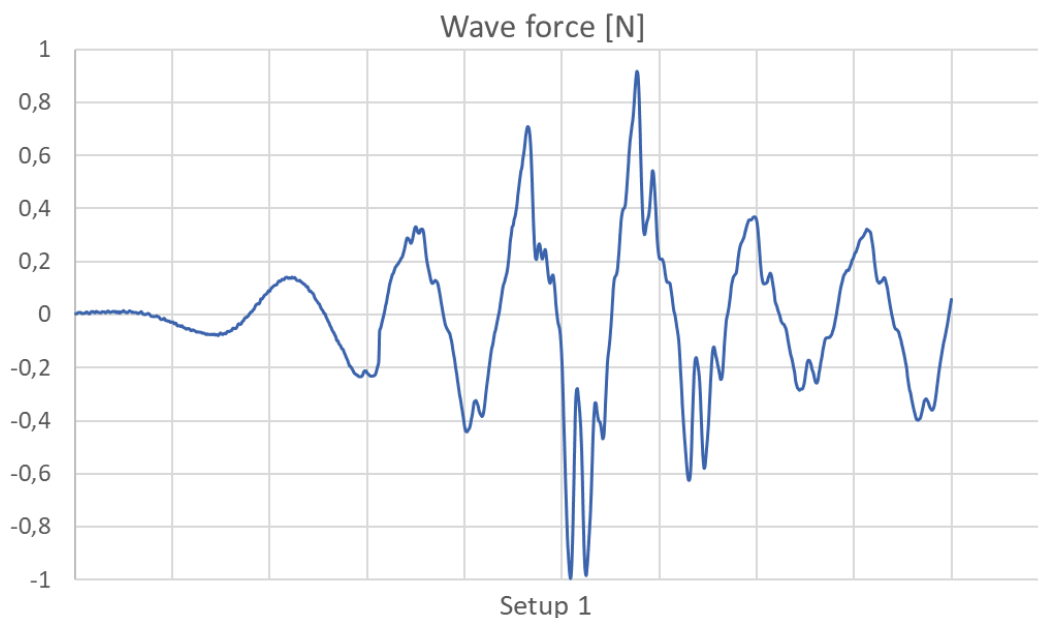
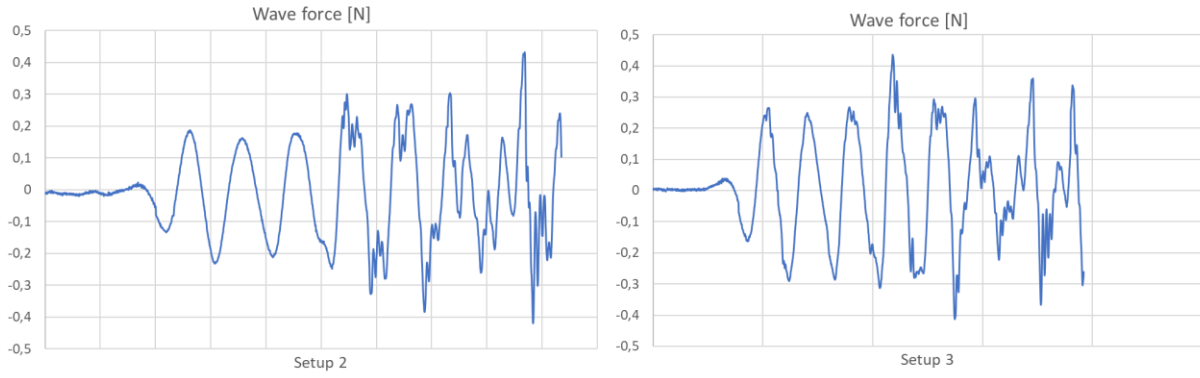**Figure 4.1** Data from reference test

4.1 Tests in wave tank

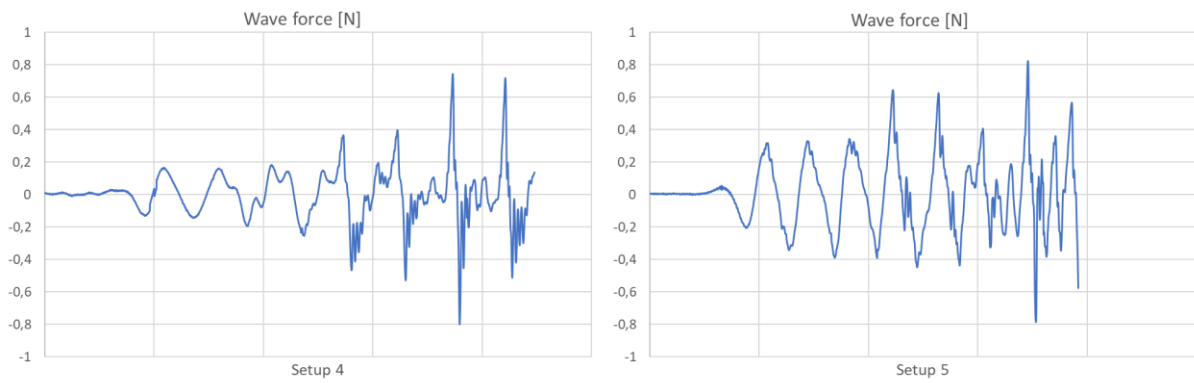**Figure 4.2** Reference test data, setup 2 and 3

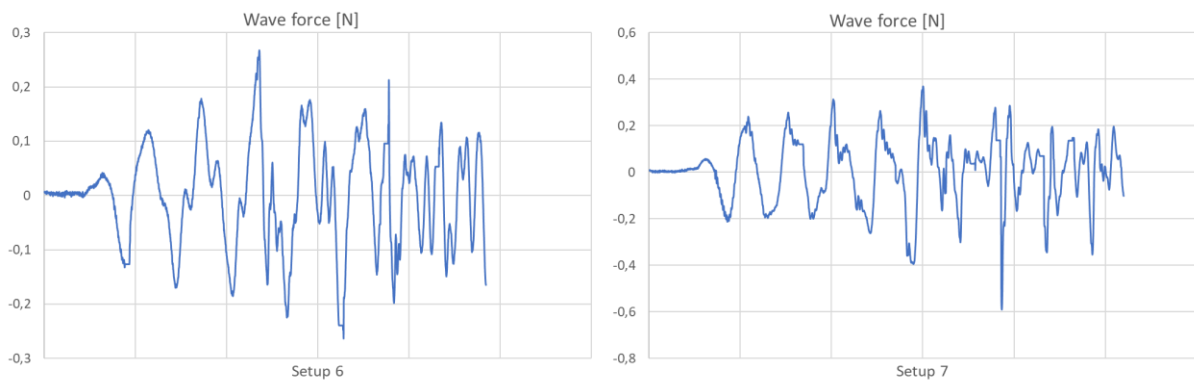**Figure 4.3** Reference test data, setup 4 and 5

Figure 4.4 Reference test data, setup 6 and 7

4.1 Tests in wave tank

From Figure 4.1 to Figure 4.4, the most relevant data from the reference tests are shown. The data gathered from the reference tests make up the basis for the experimental testing and the numerical simulations. From all of the conducted reference tests, seven different configurations were chosen to present a variety of setups. The results from the other reference tests are shown in Appendix A. From the results it is shown that the exerted wave force is quite small, with the largest value just under 1 N. This is a result of the waves not reaching the full potential as they should have if the actual height was corresponding to the input data. As the setup is now, the return waves are also being registered. This is seen at the end of the plot where the frequency is increased as a result of the incoming waves meeting the return waves.

Another variable that could affect the results is the cylinder not being completely locked in place. Wedges are used to keep the cylinder from having any yaw or pitch movement. To get a magnitude indication from the results, this is acceptable although there is room for improvement. To get more accurate results, the reference test should have been conducted after the water level was raised and the wave beach properly functioning. However, it was through these results, it was noticed that this was something that needed to be done. Based on the reference tests, the force output used for the FEM simulation and calculation is set to 0.5 N.

4.1.2 Experimental testing results

With the strain gauges calibrated and the background noise reduced to a minimum, the experimental tests started to yield applicable results. These results are a big part of the thesis as they are compared against the results for the numerical model. An important aspect with the experimental testing is how accurate results the strain gauges could provide. The results from the experimental tests are shown from Figure 4.5 to Figure 4.8.
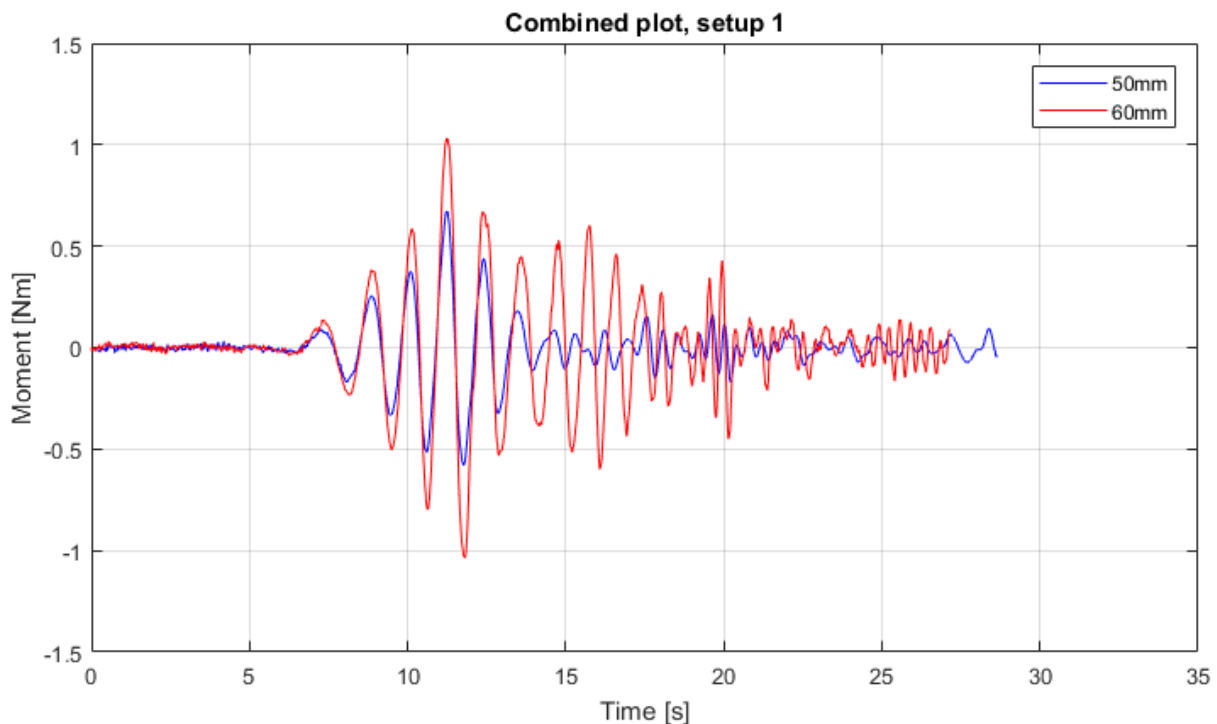

Figure 4.5 Data from experimental testing in tank
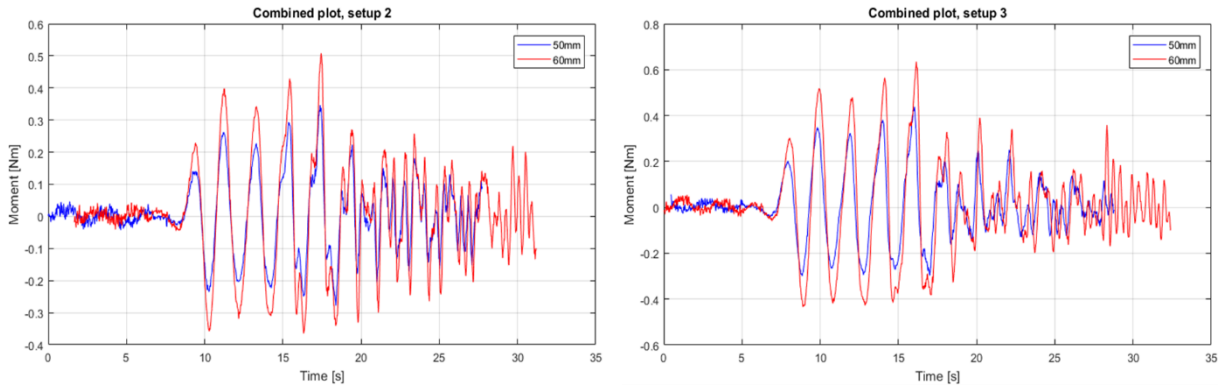
4.1 Tests in wave tank

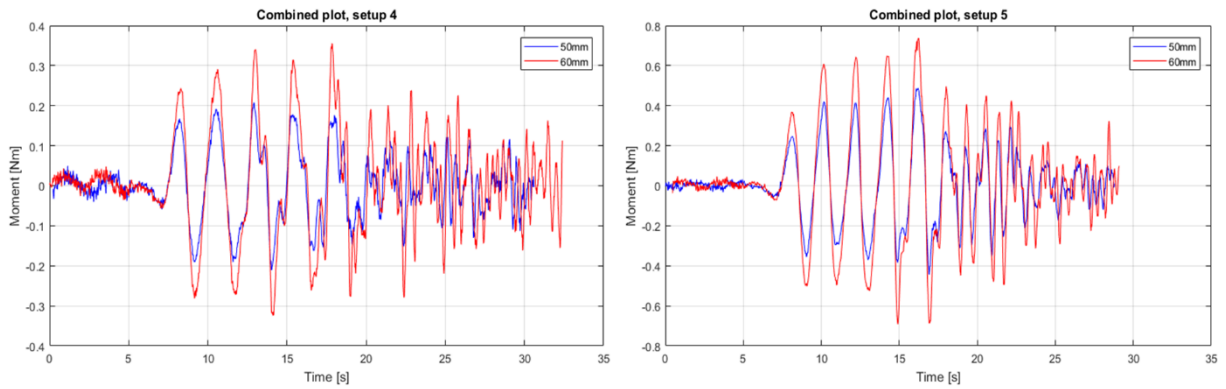**Figure 4.6** Experimental test data, setup 2 and 3

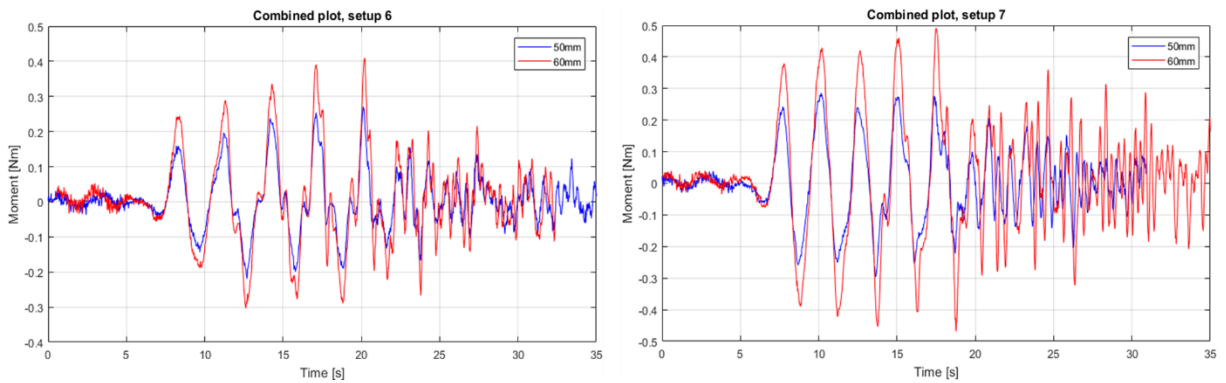**Figure 4.7** Experimental test data, setup 4 and 5

Figure 4.8 Experimental test data, setup 6 and 7

4.1 Tests in wave tank

As previously mentioned, the diameter of the cylinder is set to 60 mm. In addition to doing the tests with this setup, a cylinder with 50 mm diameter was also used. This was done to get more data to compare against, and also to see how much impact the diameter has on the results. For practical reasons, the results from both the 50 mm and 60 mm cylinder are plotted in the same graph for each of the setups. The 50 mm diameter cylinder is shown with blue curves, while the 60 mm is shown with red. This makes comparison of the various diameters easier to see. The graphs are adjusted to get the waves to overlap each other. For all the different setups, a bigger cylinder diameter yields a higher moment output. This could be a result of the waves moving more weight with the 60 mm cylinder, and thereby increases the moment, while the mounting bracket where the strain gauges are mounted is the same for both cases. The MATLAB script used to plot the graphs is found in Appendix B.

The remaining background noise is seen at the start of all the plots. Setup 4 in Figure 4.7 is one of the places it can be seen most clearly. This is due to the low values making the scaling more compact than some of the other graphs. Once the wave generator is running, the interference is gone. After the first five waves when the wave generator stops, the interference returns. All the tests are run with five waves, the additional peaks after the initial five waves are a combination of the return waves and background noise. The return waves usually occur at around 20 seconds of logging for most setups.

With the strain gauges placed on the mounting bracket, the data output is not registered as wave force directly. The data output from the strain gauges is given in [Nm]. This means that the results from the experimental tests are the moment at the strain gauges, caused by the waves hitting the cylinder. The highest value registered is in setup 1 where there is registered a value of 1 Nm. When looking at results where the data is registered as consistent even peaks, the output is in the range of 0.5 Nm.

When comparing the various setups against each other, it is noticeable that some of the parameters yield better results than the rest. The setups with the highest output values are also the ones with the shortest period. Once the period increases without the wave height also increasing, the moment output decreases. This makes sense as a higher wave with shorter intervals will have a more significant impact than a shorter and longer wave. To further increase the moment output the wave tank would need to be calibrated so it can generate waves with the actual set wave height.

4.2   Numerical simulation results

4.2.1 FEM results

For an iterative process like this has been regarding design changes, FEM has been an invaluable tool. What to highlight and explain further on a model will depend on what problem is being solved. For the cylinder, it is the exerted wave force that is the main thing affecting the model. From the applied force, results regarding displacement and stress can be derived.
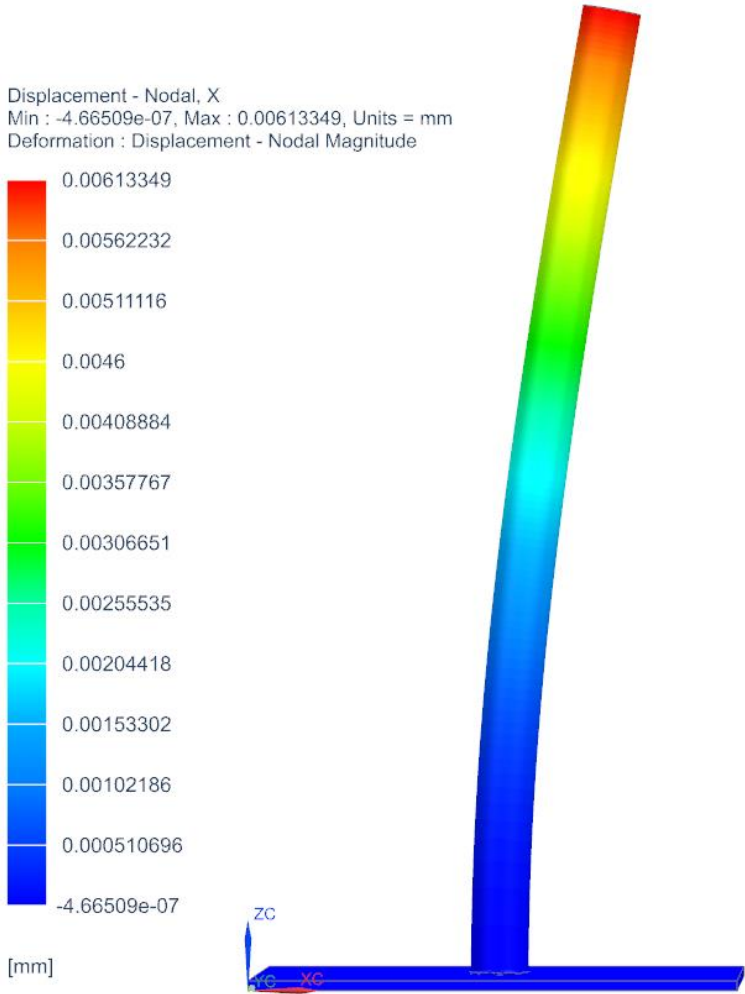

Displacement - Nodal, X
Min : -4.66509e-07, Max : 0.00613349, Units = mm
Deformation : Displacement - Nodal Magnitude

0.00613349
0.00562232
0.00511116
0.0046
0.00408884
0.00357767
0.00306651
0.00255535
0.00204418
0.00153302
0.00102186
0.000510696
-4.66509e-07

[mm]

Figure 4.9 Original design with exaggerated displacement

Since the original design had the cylinder mounted directly to the base plate, it provided a more rigid model. This could have been beneficial if not for the fact that this would be an impractical solution for changing the cylinder diameter. From the given displacement, there is no need for concern regarding structural behavior. It is this setup that mimics the control calculations.

4.2 Numerical simulation results

As seen in Figure 4.10, the model has some displacement from the exerted wave force. From the given orientation of the model, this displacement is just under 1 mm in Z-direction. Any deformation on the model is not the cylinder itself deforming, but rather the mounting bracket giving in for the applied force causing the cylinder to deviate slightly from the original position. The applied force is taken from the reference tests and set to 0.5 N. With the deformation at the mounting bracket this low, it is not necessary to apply design changes. The displacement at the top of the cylinder is also within an acceptable range.
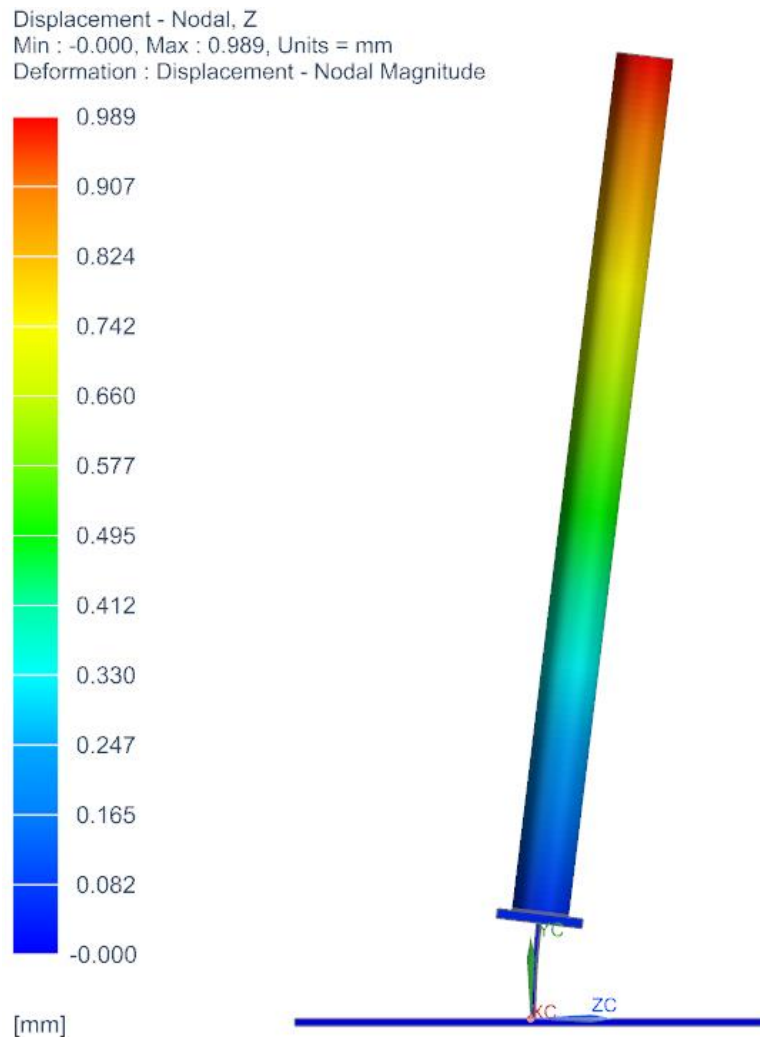
Figure 4.10 Exaggerated displacement as a result of exerted wave force

For these designs, the deformation and displacement is not a problem. If the wave generator were able to produce waves with the correct height as the input, the displacement would be more noticeable. Both of the models are showing an exaggerated view of the displacement for illustrative purposes. The color coding along the cylinder shows how the displacement gradually increases as it gets closer to the top where the force is applied.

4.2 Numerical simulation results

Deformation at the top of the flat mounting bracket is caused by the force applied to the top of the cylinder. The force makes a lever arm rotation around the bottom of the cylinder, meaning that the force on the top of the cylinder is transformed into a rotating moment at the bottom of the cylinder. The lower end of the flat mounting bracket is fixed while the rotating moment is acting on the other end. This load leads to displacement on the top of the flat mounting bracket and the whole bar deforms. The stress can be used to derive the strain by using the Young's modulus. Strain is defined as stress divided by Young's modulus and is thereby dimensionless. The Young's modulus for the used aluminum is 73 GPa. Using this along with the stress from Figure 4.11 and Figure 4.12, the strain is found to be $5.78 \cdot 10^{-5}$. From the figures, it is shown that stress concentrations only occur at the welding edges at the top and bottom of the flat bar, far away from the strain gauges.
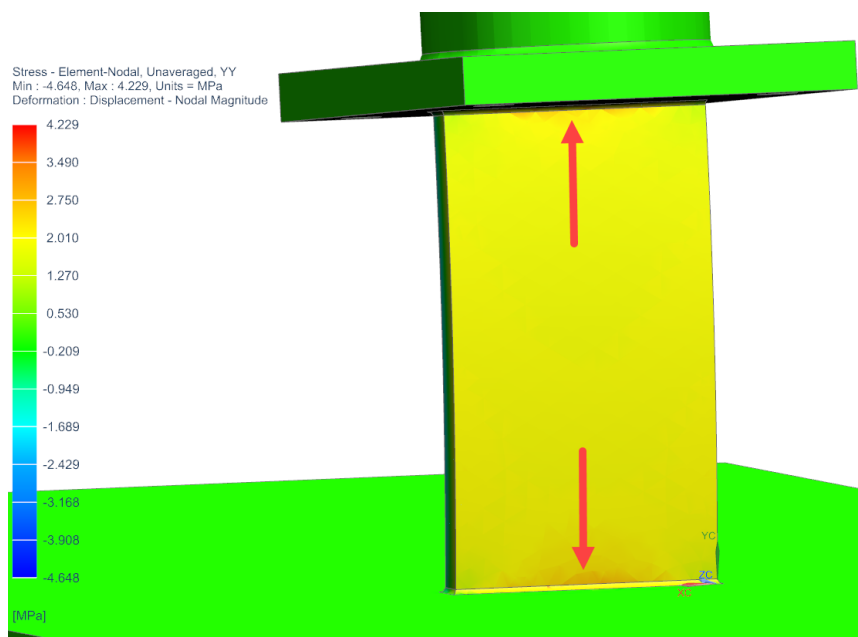
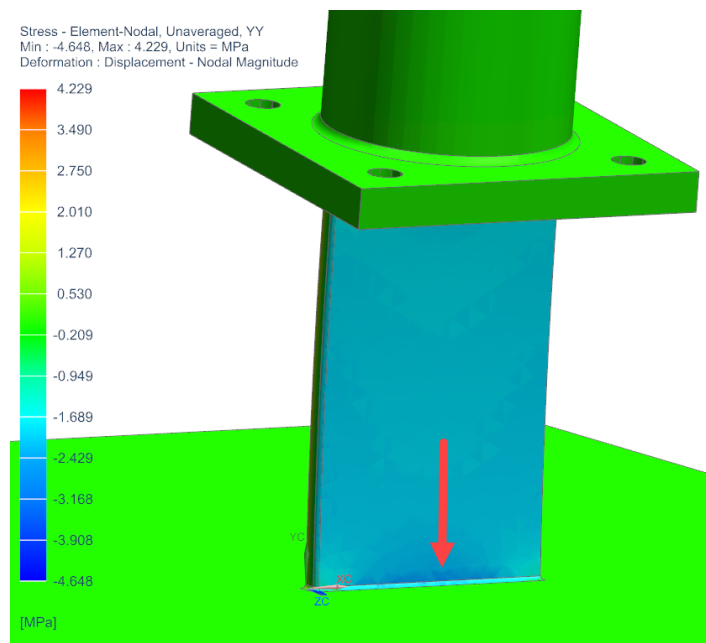**Figure 4.11** Tensile stress on the mounting bracket

Figure 4.12 Compressive stress on mounting bracket

4.2.2 Analytical model results

In addition to measuring the deflection on the cylinder with the numerical model, the analytical approach is used to verify the results and setup. The process of calculating the displacement is described in subchapter 3.3.2. Inserting the variables in equation 3.2 and 3.3 gives the displacement for the cylinder if it were attached directly to the base plate without any intermediate links.

$$I = \frac{\pi}{64}(0.06^4 \, m^4 - 0.048^4 \, m^4) = 3.76 \cdot 10^{-7} \, m^4 \qquad 4.1$$

Moment of inertia is calculated by using the outer and inner diameter of the cylinder.

$$y = \frac{0.5 \, N \cdot 1^3 \, m^3}{3 \cdot 73\,119 \cdot 10^6 \, \frac{N}{m^2} \cdot 3.76 \cdot 10^{-7} \, m^4} = 6.06 \cdot 10^{-6} \, m = 0.0061 \, mm \qquad 4.2$$

Equation 4.2 shows how the displacement on the first design setup is calculated. The used Young's modulus for aluminum is for a temperature of 20°C. By using the same parameters as the numerical setup on the first design and the same force as found in the reference tests, it is possible to verify if the FEM procedure is done correctly. Both the analytical calculation and FEM simulation is done with the force applied at the end of the cylinder. To further control the setup, the same calculations can be done on the final design. It would then have to be taken into consideration that a rectangular cross-section has to be used instead of a cylindrical cross-section when calculating moment of inertia.

Morison equation can be used to estimate the wave force on the cylinder. The Morison equation was set up and calculated by using MATLAB. From the equation, it was found that the estimated force at the free surface level is 0.015 N. This value is for a certain point on the cylinder as the Morison equation calculates a specific point. The MATLAB script used to calculate the force estimation from the wave on the monopile can be seen in Appendix B.

4.2.3 Computational Fluid Dynamic results

With the CFD model configured, the cylinder is simulated for the various setups. To get the same results as the experimental tests, the same parameters are used. This includes using the actual wave height and looking at the same number of waves. The plotted data output for the numerical simulation is given in [N]. This force is registered directly where the wave hits the cylinder. The horizontal axis shows the physical time and not the simulation time used.
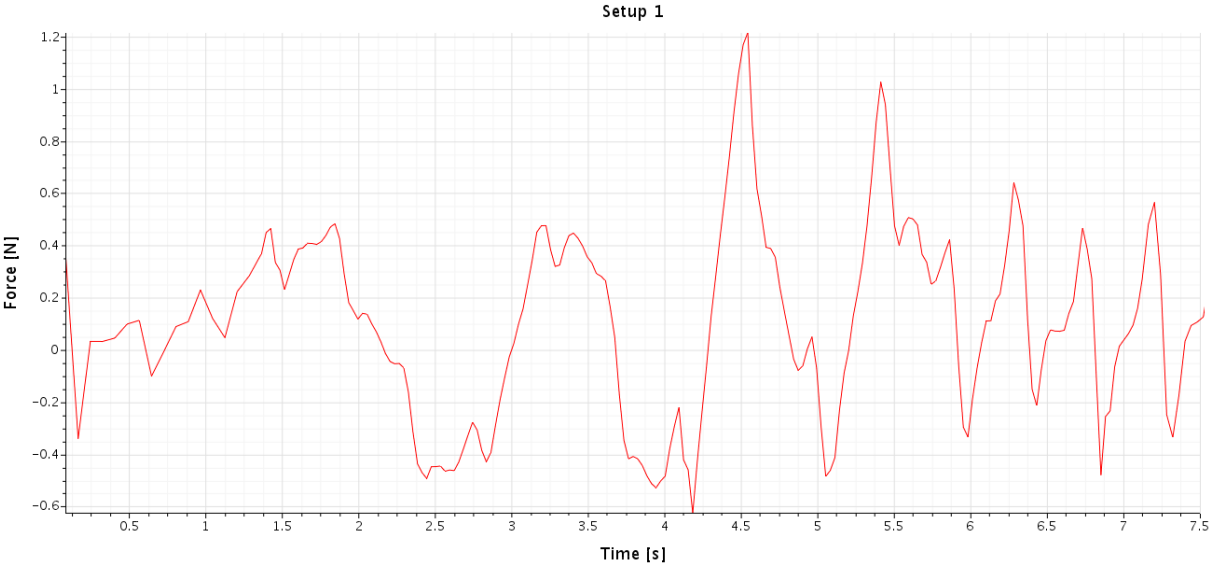

Figure 4.13 CFD simulation data, setup 1
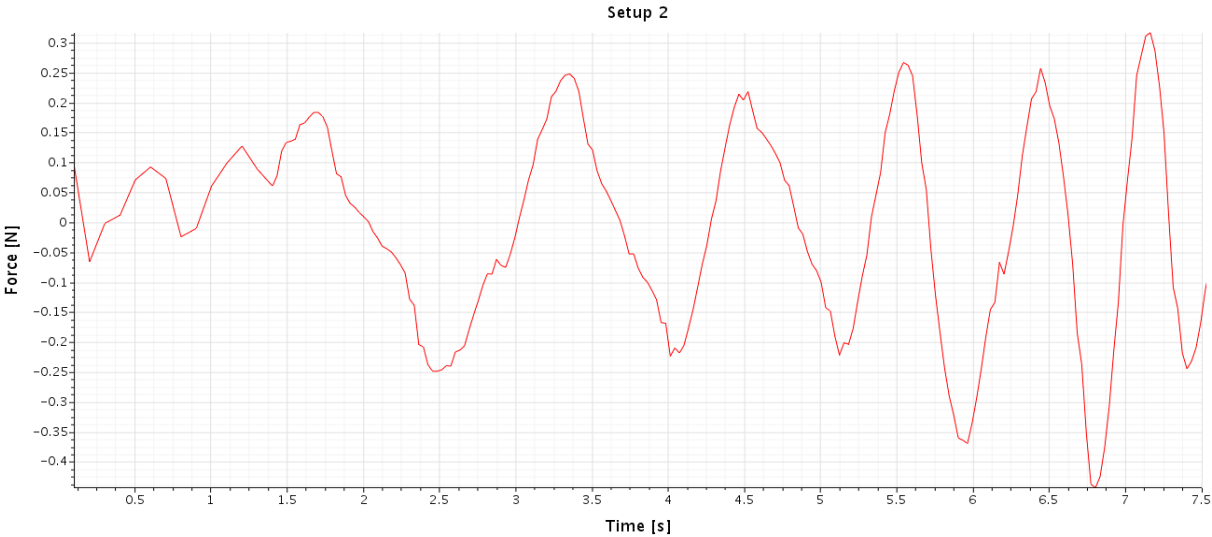
Figure 4.14 CFD simulation data, setup 2

4.2 Numerical simulation results
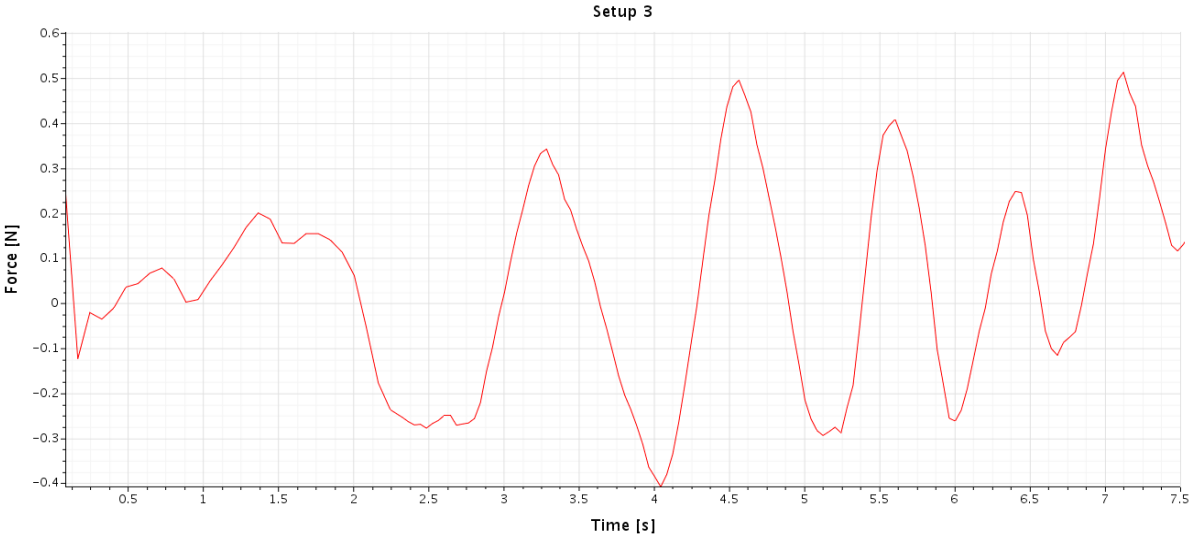
Figure 4.15 CFD simulation data, setup 3
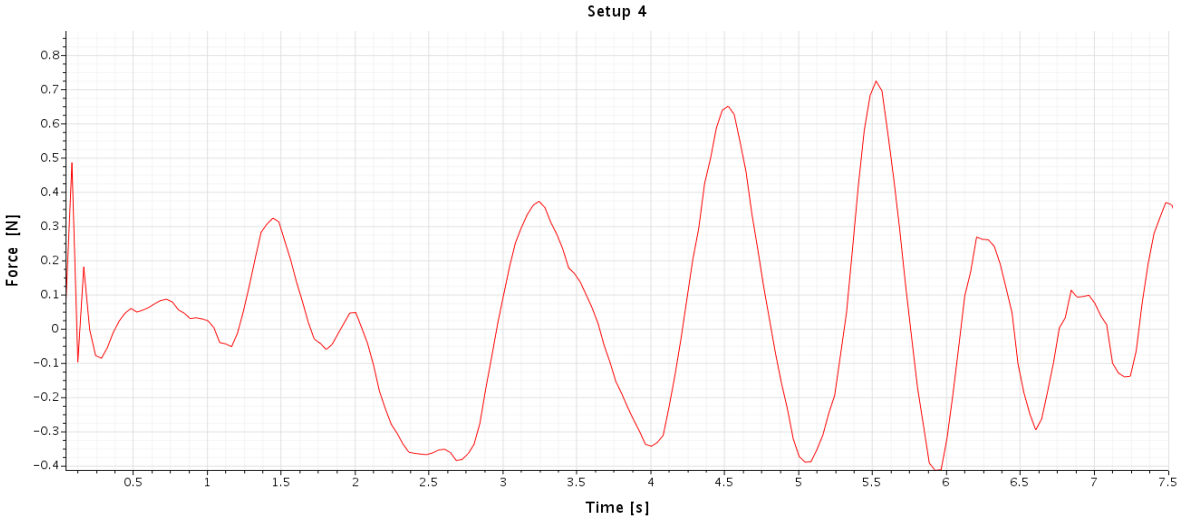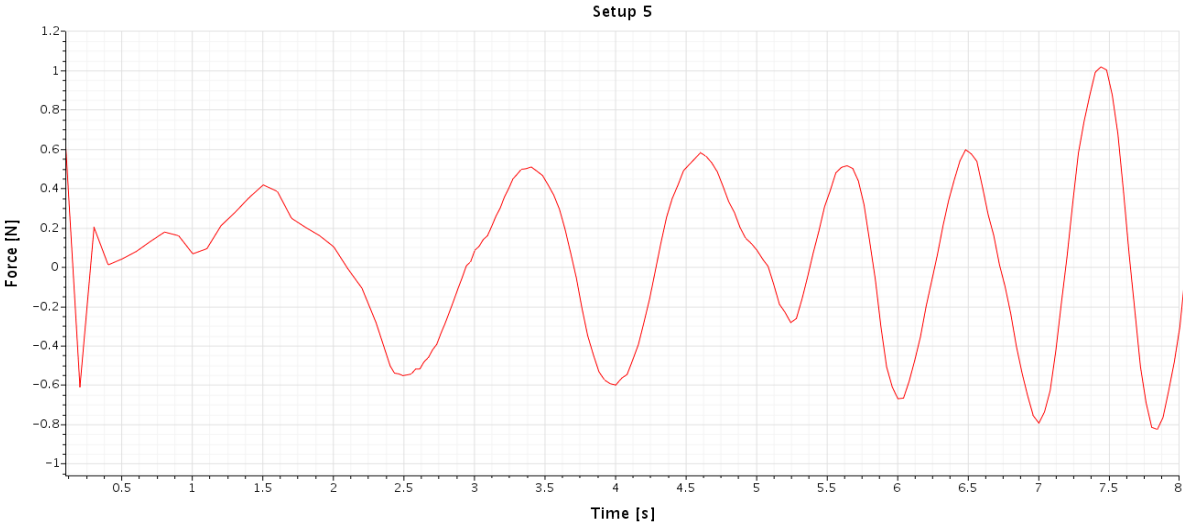

Figure 4.16 CFD simulation data, setup 4

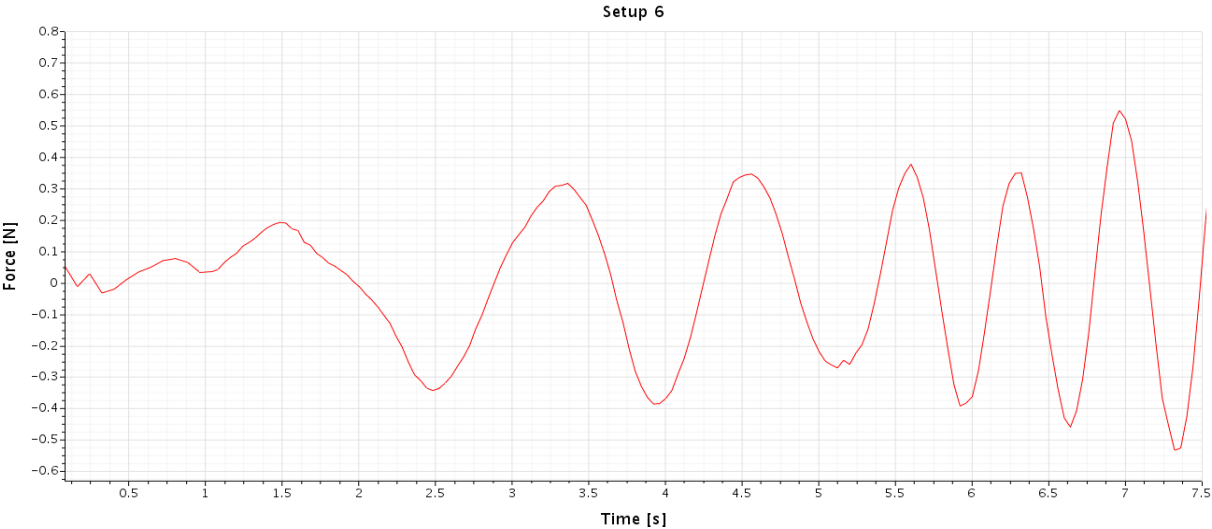**Figure 4.17** CFD simulation data, setup 5

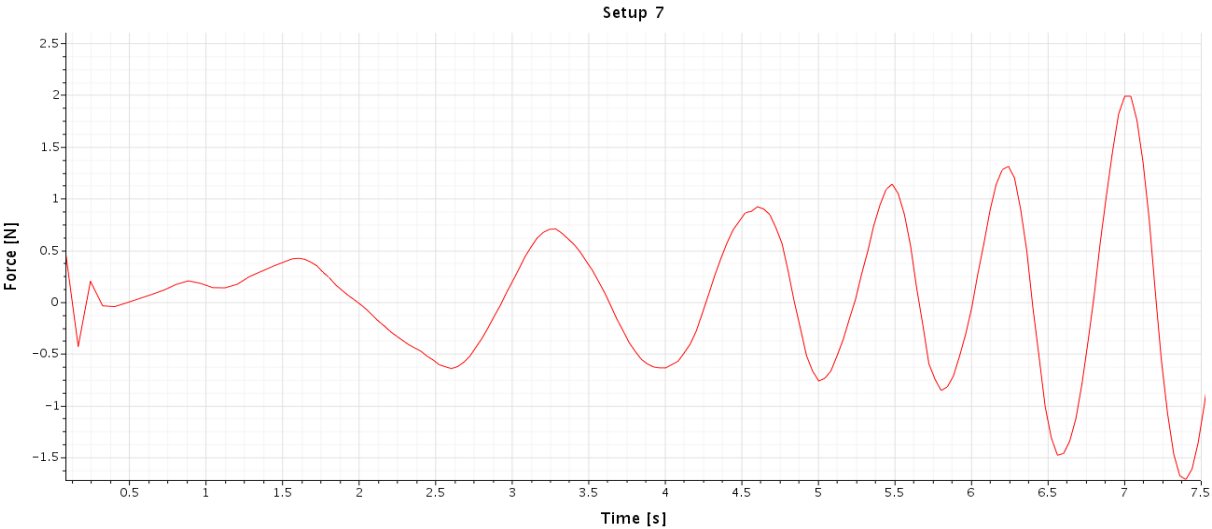**Figure 4.18** CFD simulation data, setup 6

Figure 4.19 CFD simulation data, setup 7

4.2 Numerical simulation results

From Figure 4.13 to Figure 4.19, the results from the CFD simulation are shown. The figures show that the graphs do not develop properly. There are few places where the curves represent even waves. This is most likely due to a bad CFD setup. Some of this can also be related to limited computational power. To improve the results, a better mesh is the most likely parameter to have a significant effect. A revision of the other parameters, such as solver configurations is also needed. When comparing the period from Table 3.3 with the graphs, it can be seen that there is some deviation. The period in the graphs does not match up with the set input value.

An objective with the research is to use the same parameters for the various tests. Since the experimental tests are limited to five waves per test by the wave generator, it is the first five waves that are the most relevant for the numerical tests. Using more than five waves would make the results irrelevant as there is no basis for comparison.

When looking at the setups, the waves have some variation in force output. The relevant force output from the various setups ranges from 0.25 N to 1.2 N. To find the effect from the waves on the same point as the strain gauges, the force is converted to moment. This is done by multiplying the force output with the depth of the water level. Since the water depth is close to 1 m, the moment is relatively unchanged from the force output. The variation is that the moment has a slightly lower value than the force output. All of the setups shown in the graphs are simulated with about seven seconds of physical time.
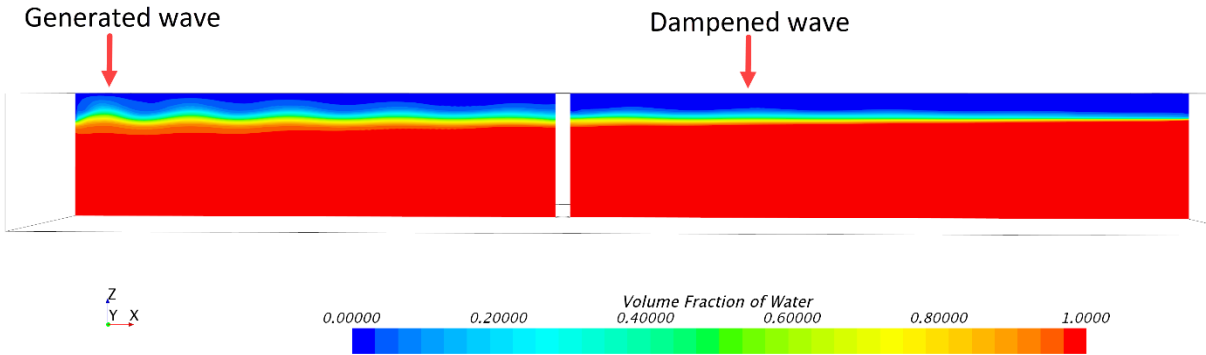

Figure 4.20 VOF wave development, setup 5

Figure 4.20 shows how waves are dampened over time as they move along the X-direction. With a higher resolution on the meshing, the waves would not dampen out so quickly. The mesh used for the simulation is good enough to visualize the waves and show how they develop. However, for a more accurate representation, a finer mesh is needed. This is a limitation with the computational power available. A more accurate model could be simulated with more computational power but for this research, a compromise was made. The cylinder is also contributing to slowing down the waves and further increase the dampening. The wave development for the other setups and the velocity flow around the cylinder can be seen in Appendix C.

5 Conclusion and future work

5.1 Conclusion

This research is focused on investigating the effect of waves on coastal structures. More precisely, the cylindrical base structure of wind turbines. To investigate the effects, numerical models, experimental tests and analytical solutions are used. The purpose of using multiple methods in the research is to have some degree of validation for the results.

Virtually developing the cylinder has been useful to change design parameters along the way. FEM analysis has also been used to asses the structural integrity of the structure and to visualize any displacement from the external force applied. Virtually developing the model has been an invaluable tool for the design process.

One of the objectives of the research is to develop a numerical test tank. To develop the numerical tank, computational fluid dynamics is used. CFD is used to model the cylinder in a virtual tank, with the same wave configurations as the experimental tests. The limitations of the research are related to the size of the wave tank used for the experimental tests. There is also a limitation on the quantity of generated waves, as it were not possible to generate more than five waves per test.

With the correct configurations, it is possible to use the numerical model for simulation-based design of structures in waves. The numerical model can be used to assess how the structure will behave with an external force applied. The force plot from the simulations shows that the exerted wave force is quite low and will not have any significant effect on the cylinder. It is also shown how the flow behaves around the cylinder.

In addition to the numerical simulations, experimental tests are conducted. The experimental tests rely on sensors to register the data output. The reference test uses the available sensor on the towing wagon in the tank, while the experimental test has strain gauges installed on the cylinder. How reliable the data output is, depends on the sensor quality, but also sensor calibration. The sensors are calibrated using known loads for both the reference test and the actual test in the tank. Judging by the data output after the calibration, it can be determined that the sensors provide applicable data. This can be seen in the results from the experimental test data where the sensor registers a clear oscillating pattern for each wave.

As mentioned, this research is based on various methods of extracting data on the same cause. How the results of these methods add up is essential for the validity of the research. From the gathered results on the various methods, it is shown that the data output yields similar values. Some slight variation does occur as a result of the exact parameters being challenging to replicate. This variation is also related to the CFD setup not being adequate. The research has potential, but more work is still needed for any direct validation.

5.2 Future work

Future research into this topic should consider the benefits of redoing the experimental tests with a calibrated wave tank to get waves with the correct height. With the wave height matching the input data, it would most likely be possible to get more variety in data output. It should also be added a 70 mm cylinder to the experimental test, to research the effect of chosen diameter further. A better wave tank with fewer limitations would also benefit the research.

The numerical model should be improved to increase the accuracy of the CFD results. It is especially the mesh that could use more work. This again comes down to available computational power. With enough computational power to improve the mesh, it would be possible to simulate a more detailed wave.

To get an indication of what this research means for a full-scale scenario, Froude scaling should be applied to the results. This would give the research a more realistic view of what forces to expect from waves. It is also easier to understand the magnitude of the forces when looked at in full scale. Using Froude scaling is a way of tracking the research back to the original topic, offshore wind turbines.

6 References

AkerSolutions. (2018). *Subsea Production Systems*. Hentet 11 22, 2018 fra akersolutions.com: https://akersolutions.com/what-we-do/products-and-services/subsea-production-systems/

American Geosciences Institute. (2018). *What are the advantages and disadvantages of offshore wind farms?* Hentet 11 23, 2018 fra www.americangeosciences.org: https://www.americangeosciences.org/critical-issues/faq/what-are-advantages-and-disadvantages-offshore-wind-farms

American Oil & Gas Historical Society. (2014). *Offshore Petroleum History*. Hentet 11 22, 2018 fra aoghs.org: https://aoghs.org/offshore-history/offshore-oil-history/

Bureau of Ocean Energy Management. (2016, 05). *Renewable Energy on the Outer Continental Shelf*. Hentet 11 23, 2018 fra www.boem.gov: https://www.boem.gov/Offshore-Wind-Energy/

Cuellar, P. (2012, 1). *Wind Turbine Dimensions*. Hentet 3 2019 fra researchgate.net: https://www.researchgate.net/figure/Approximate-dimensions-of-a-5-MW-offshore-wind-turbine-with-monopile-foundation-and-order_fig1_233924820

DNV GL. (2018). *Electrifying the future*. Hentet 11 2018 fra dnvgl.com: https://www.dnvgl.com/technology-innovation/broader-view/electrifying-the-future/third-generation-wind-power.html

Field, A. (2017, 10 30). *What is the difference between implicit and explicit unsteady simulation approaches ?* Hentet 05 20, 2019 fra thesteveportal.plm.automation.siemens.com: https://thesteveportal.plm.automation.siemens.com/articles/en_US/FAQ/What-is-the-difference-between-implicit-and-explicit-unsteady-simulation-approaches?fbclid=IwAR23NGeo5-H8uEkIMUdeVdgy7FUYeLqboPB-c8qfbdEe11dOz9MKYSgiZMc

Fowler, M. J., Kimball, R. W., Dale, T. A., & Goupee , A. J. (2013, 06). *Design and Testing of Scale Model Wind Turbines for Use in Wind/Wave Basin Model Tests of Floating Offshore Wind Turbines.* Hentet 11 26, 2018 fra www.researchgate.net: https://www.researchgate.net/publication/267607061_Design_and_Testing_of_Scale_Model_Wind_Turbines_for_Use_in_WindWave_Basin_Model_Tests_of_Floating_Offshore_Wind_Turbines

Fredsøe, B. M. (2006). *Hydrodynamics around cylindrical structures* (Revised edition. utg.). Singapore: World Scientific Publishing Co. Pte .Ltd. Hentet 2018 fra https://bibsys-almaprimo.hosted.exlibrisgroup.com/primo-explore/fulldisplay?docid=TN_worldsbk10.1142%2F6248&context=PC&vid=NTNU_UB&lang=no_NO&search_scope=default_scope&adaptor=primo_central_multiple_fe&tab=default_tab&query=any,contains,Hydrodynamics%20A

HBM. (2019). *HBM Instructions for use.* Hentet 05 14, 2019 fra ase.au.dk:
http://ase.au.dk/fileadmin/www.ase.au.dk/Filer/Laboratorier_og_vaerksteder/Inst
rument_Depotet/Kemikalier/TDS_-_SG_250.pdf

IEE, F. (2018). *Distance to shore and water depth*. Hentet 11 19, 2018 fra
http://windmonitor.iee.fraunhofer.de:
http://windmonitor.iee.fraunhofer.de/windmonitor_en/4_Offshore/2_technik/2_Ku
estenentfernung_und_Wassertiefe/

Iska, K. (2017, 10 25). *Navier-Stokes equation*. Hentet 11 24, 2018 fra
/medium.com/iskakaushik: https://medium.com/iskakaushik/navier-stokes-
equation-for-a-dummies-15421f15af18

John. (2011, 08 5). *Strain Gauge*. Hentet 05 15, 2019 fra instrumentationtoday.com:
http://www.instrumentationtoday.com/strain-gauge/2011/08/

Kalaskar, K. (2018, 11 29). *What are the best settings for a VOF wave model simulation?*
Hentet 05 15, 2019 fra thesteveportal.plm.automation.siemens.com:
https://thesteveportal.plm.automation.siemens.com/articles/en_US/FAQ/What-
are-the-best-settings-for-a-VOF-wave-model-simulation

Kundu, P. K., Cohen, I. M., & Dowling, D. R. (2012). *Fluid Mechanics* (Fifth edition. utg.).
Oxford: Elsevier. Hentet 11 24, 2018

Lindqvist, P. (2005, 08). Notes on the p-Laplace equation. Trondheim, Norway. Hentet 11
23, 2018

Midling, A. S. (2015, 11 25). *Norway's coast challenging for offshore wind turbines*.
Hentet 11 23, 2018 fra sciencenordic.com/norway:
http://sciencenordic.com/norway%E2%80%99s-coast-challenging-offshore-wind-
turbines

National Instruments Corporation. (1998, 08). *Strain Gauge Measurement - A Tutorial.*
Hentet 05 16, 2019 fra http://elektron.pol.lublin.pl:
http://elektron.pol.lublin.pl/elekp/ap_notes/NI_AN078_Strain_Gauge_Meas.pdf

Nelson, B. (2017, 10 10). *Offshore wind farms could power all of human civilization*.
Hentet 11 20, 2018 fra mnn.com: https://www.mnn.com/earth-
matters/energy/stories/offshore-wind-farms-can-alone-power-all-human-
civilization

Nichols, B. D., & Hirt, C. W. (1981). *Journal of Computational Physics* (Volume 39 Issue
1. utg.). Los Alamos: Elsevier. Hentet 11 24, 2018

NTNU. (2018). *Maritime Engineering*. Hentet 11 2018 fra ntnu.edu:
https://www.ntnu.edu/studies/msnmme/study-tracks

OMEGA. (2019). *Measuring Circuits*. Hentet 05 15, 2019 fra omega.co.uk:
https://www.omega.co.uk/literature/transactions/volume3/strain2.html

Physicskey. (2017, 12 5). *Simple Harmonic Wave Function and Wave Equation*. Hentet
11 21, 2018 fra www.physicskey.com: https://www.physicskey.com/35/simple-
harmonic-wave-function-and-wave-equation

Piehl, H. (2017, 9). Computer Aided Engineering Course. *Lecture notes*. Ålesund. Hentet
2019

Piehl, H. (2018, 9). Scientific theory and methods course . Ålesund, Norway. Hentet 10 2018

Prokos, C. (2019, 1 11). *Introduction to Solidworks simulation webinar: What is Finite Element Analysis?* Hentet 5 4, 2019 fra fisherunitech.com: https://www.fisherunitech.com/blog/introduction-solidworks-simulation-webinar-finite-element-analysis

SimWiki. (2018). *What is CFD | Computational Fluid Dynamics?* Hentet 11 24, 2018 fra www.simscale.com: https://www.simscale.com/docs/content/simwiki/cfd/whatiscfd.html

Singh, G. (u.d.). *Short Introduction to Finite Element Method .* Hentet 11 23, 2018 fra www.idi.ntnu.no: http://www.idi.ntnu.no/~elster/tdt24/tdt24-f09/gagan-fem.pdf

Skogsfjord, M. (2014, 8 24). *Finite Element Method – Lesson 1*. Hentet 11 2018 fra nxportalen.com: http://nxportalen.com/blog/2014/08/26/finite-element-method-lesson-1/

Suja-Thauvin, L., Krokstad, J. R., & Frimann-Dahl, J. F. (2016). *Maximum Loads on a One Degree of Freedom Model-Scale Offshore Wind Turbine .* Trondheim : Elsevier. Hentet 11 26, 2018 fra https://ac.els-cdn.com/S1876610216308438/1-s2.0-S1876610216308438-main.pdf?_tid=661fa880-fd7c-467c-a59c-27a91824ba27&acdnat=1543241862_211168d41a29c6be601382ee878cc2c9

Transocean. (2018). *Rig Types*. Hentet 11 22, 2018 fra www.deepwater.com: https://www.deepwater.com/our-fleet/rig-types

Weisstein, E. W. (2018). *Finite Volume Method*. Hentet 11 24, 2018 fra /mathworld.wolfram.com: http://mathworld.wolfram.com/FiniteVolumeMethod.html

Wärtsilä. (2018). *MODEL TESTS*. Hentet 11 25, 2018 fra www.wartsila.com: https://www.wartsila.com/encyclopedia/term/model-tests

Appendix A – Reference test results

In addition to the seven test setups used for the various testing, there were done more reference tests. These are shown in the following figures. These tests are labeled with the wave height and period set in the wave generator. It is worth noting that the set wave height does not correspond to the actual wave heights produced by the wave generator.
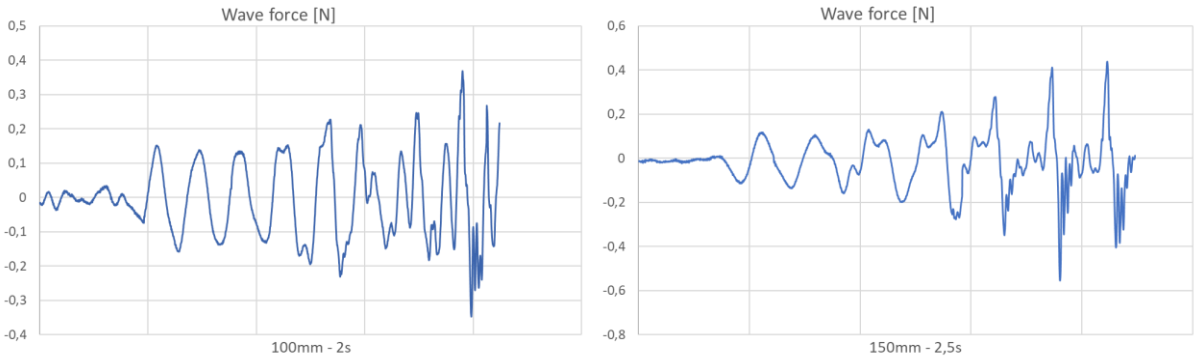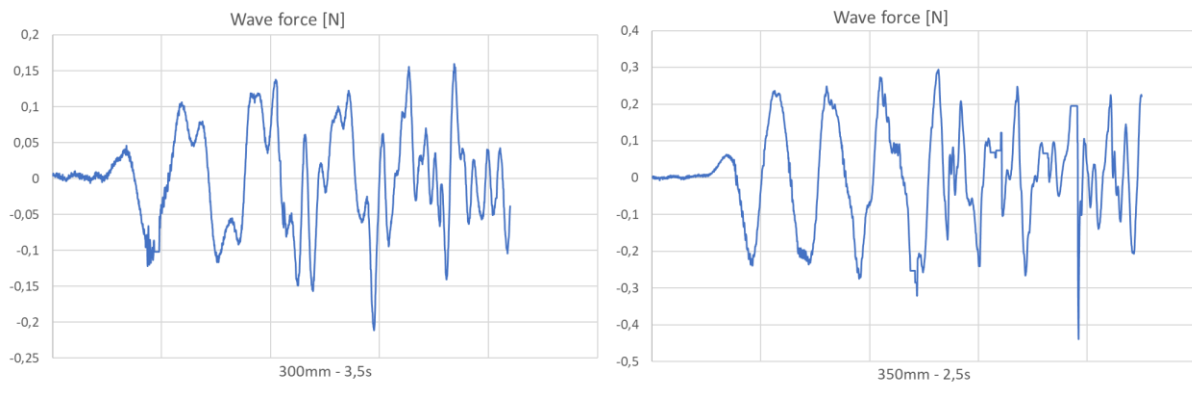

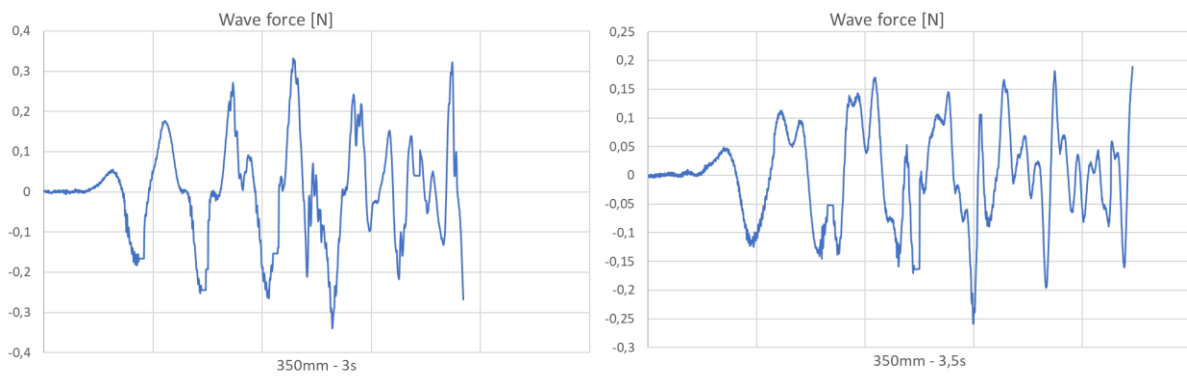**Appendix Figure 1** Reference test data 100 mm and 150 mm input value
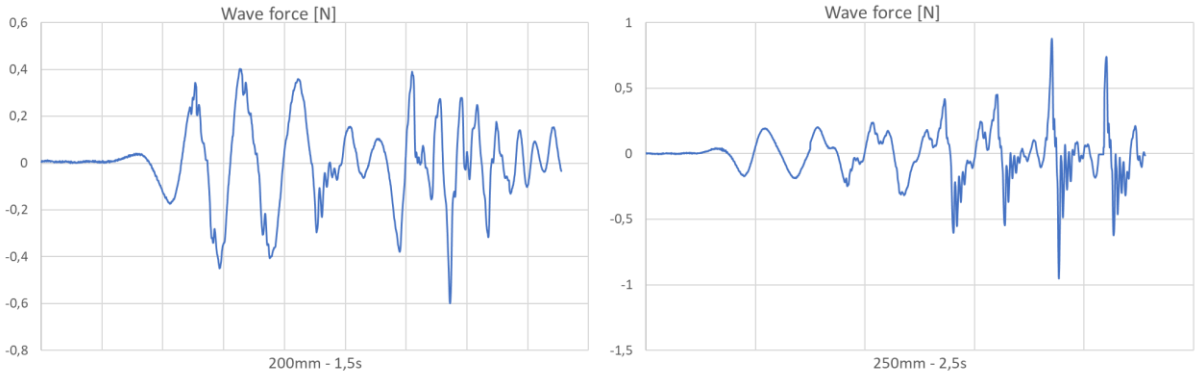
Appendix Figure 2 Reference test data 200 mm and 250 mm input value
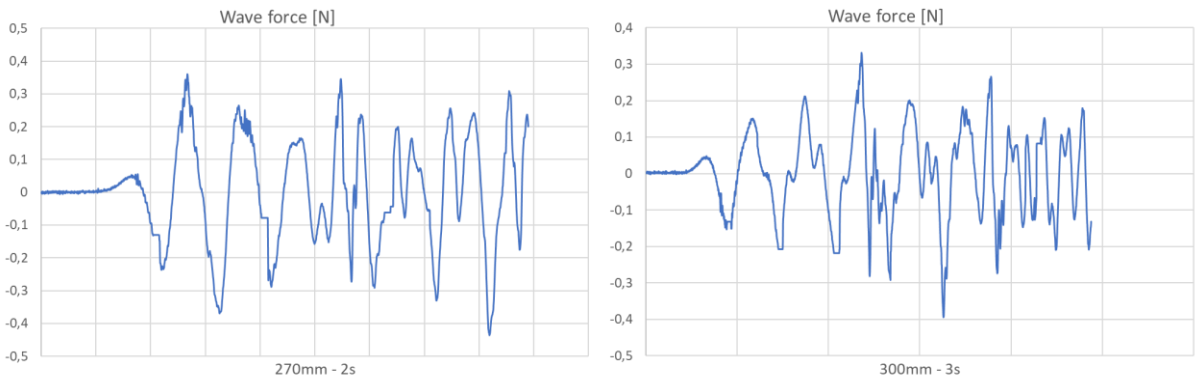
Appendix Figure 3 Reference test data 270 mm and 300 mm input value

Appendix Figure 4 Reference test data 300 mm and 350 mm input value

Appendix Figure 6 Reference test data 350 mm with 3 s and 3.5 s period input
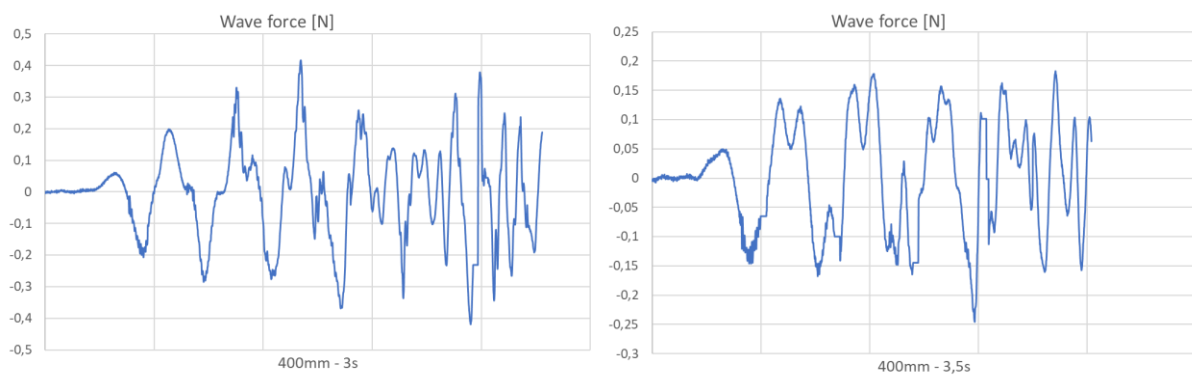
Appendix Figure 5 Reference test data 400 mm with 3 s and 3.5 s period input

Appendix B – MATLAB scripts

Script for calculating the Morison equation

```matlab
%% Morison Equation

clc

rho = 1000;      % Density
Cm = 2.0;        % Mass coefficient
Cd = 1.2;        % Drag coefficient - between 1.0-1.4
d = 0.06;        % Outer cylinder diameter in m

% Wave information

H = 0.05;               % Wave height in m
T = 2.0;                % Wave periode in s
A = H/2;                % Wave height in m
w = 2*pi/T;             % Angular frequency
L = 9.81/(2*pi)*T^2;    % Wave length
k = 2*pi/L;             % Wave number
z = -0.2;               % Depth where z is free surface level


% Wave velocity

u = A*w*exp(k*z)*cos(0)   % Wave velocity
U = A*w^2*exp(k*z)*1      % Particle velocity, Replacing Sin with 1



% Force calculation

% Force on cylinder in a specific point


dF = Cm*rho*(pi*d^2/4)*U*d*z+Cd*d*0.5*rho*u^2*d*z
fun = @(z) Cm.*rho.*(pi*d.^2/4).*(A.*w.^2.*exp(k.*z)*1).*d.*z...
     +Cd.*d.*0.5.*rho.*(A.*w.*exp(k.*z).*cos(0)).^2.*d.*z;

Fint = integral(fun,-0.5,0)    % Integral of whole cylinder length
% fplot(Fint)
% xlim([0 5])
% ylim([-0.5 0.5])




u = 0.0642
U = 0.2018
dF = -0.0155
Fint = -0.0084
```

Script for plotting the data from the experimental test

```matlab
%% Both cylinder diameters plotted in same graph
clc
close all;
set(0,'DefaultFigureWindowStyle','docked')


Setup1_50mm = xlsread ('Setup1_50mm.XLS');        % Setup 1
time1_50mm = smooth (Setup1_50mm (:,1));
force1_50mm = smooth (Setup1_50mm (:,3));

Setup1_60mm = xlsread ('Setup1_60mm.XLS');
time1_60mm = smooth (Setup1_60mm (:,1));
force1_60mm = smooth (Setup1_60mm (:,3));

timestart1 = 20;                                  % Adjust the time delay
newtime1_50mm = time1_50mm(timestart1:end);
newforce1_50mm = force1_50mm(1:length(newtime1_50mm));

figure
plot (newtime1_50mm,newforce1_50mm, 'color' , 'blue')
hold on
plot (time1_60mm, force1_60mm, 'color', 'red')
% plot (time1_60mm, force1_60mm, 'color', 'red')Plotted line without delay
title ('Combined plot, setup 1')
xlabel('Time [s]')
ylabel('Moment [Nm]')
legend({'50mm' , '60mm'})
xlim([0,35]);
grid on
hold off




Setup2_50mm = xlsread ('Setup2_50mm.XLS');        % Setup 2
time2_50mm = smooth (Setup2_50mm (:,1));
force2_50mm = smooth (Setup2_50mm (:,3));

Setup2_60mm = xlsread ('Setup2_60mm.XLS');
time2_60mm = smooth (Setup2_60mm (:,1));
force2_60mm = smooth (Setup2_60mm (:,3));

timestart2 = 170;                                 % Adjust the time delay
newtime2_60mm = time2_60mm(timestart2:end);
newforce2_60mm = force2_60mm(1:length(newtime2_60mm));

figure
plot (time2_50mm, force2_50mm, 'color', 'blue')
hold on
% plot (time2_60mm, force2_60mm, 'color', 'red') Plotted line without delay
plot (newtime2_60mm,newforce2_60mm, 'color' , 'red')
title ('Combined plot, setup 2')
xlabel('Time [s]')
ylabel('Moment [Nm]')
legend({'50mm' , '60mm'})
xlim([0,35]);
grid on
hold off
```

```matlab
Setup3_50mm = xlsread ('Setup3_50mm.XLS');          % Setup 3
time3_50mm = smooth (Setup3_50mm (:,1));
force3_50mm = smooth (Setup3_50mm (:,3));

Setup3_60mm = xlsread ('Setup3_60mm.XLS');
time3_60mm = smooth (Setup3_60mm (:,1));
force3_60mm = smooth (Setup3_60mm (:,3));

timestart3 = 50;                                    % Adjust the time delay
newtime3_50mm = time3_50mm(timestart3:end);
newforce3_50mm = force3_50mm(1:length(newtime3_50mm));

figure
plot(newtime3_50mm, newforce3_50mm, 'color', 'blue')
hold on
plot (time3_60mm, force3_60mm, 'color', 'red')
% plot (time3_60mm, force3_60mm, 'color', 'red')Plotted line without delay
title ('Combined plot, setup 3')
xlabel('Time [s]')
ylabel('Moment [Nm]')
legend({'50mm' , '60mm'})
xlim([0,35]);
grid on
hold off




Setup4_50mm = xlsread ('Setup4_50mm.XLS');          % Setup 4
time4_50mm = smooth (Setup4_50mm (:,1));
force4_50mm = smooth (Setup4_50mm (:,3));

Setup4_60mm = xlsread ('Setup4_60mm.XLS');
time4_60mm = smooth (Setup4_60mm (:,1));
force4_60mm = smooth (Setup4_60mm (:,3));

timestart4 = 25;                                    % Adjust the time delay
newtime4_50mm = time4_50mm(timestart4:end);
newforce4_50mm = force4_50mm(1:length(newtime4_50mm));

figure
plot (newtime4_50mm, newforce4_50mm, 'color', 'blue')
hold on
plot (time4_60mm, force4_60mm, 'color', 'red')
% plot (time4_60mm, force4_60mm, 'color', 'red') Plotted line without delay
title ('Combined plot, setup 4')
xlabel('Time [s]')
ylabel('Moment [Nm]')
legend({'50mm' , '60mm'})
xlim([0,35]);
grid on
hold off
```

```matlab
Setup5_50mm = xlsread ('Setup5_50mm.XLS');          % Setup 5
time5_50mm = smooth (Setup5_50mm (:,1));
force5_50mm = smooth (Setup5_50mm (:,3));

Setup5_60mm = xlsread ('Setup5_60mm.XLS');
time5_60mm = smooth (Setup5_60mm (:,1));
force5_60mm = smooth (Setup5_60mm (:,3));

timestart5 = 50;                                    % Adjust the time delay
newtime5_60mm = time5_60mm(timestart5:end);
newforce5_60mm = force5_60mm(1:length(newtime5_60mm));

figure
plot (time5_50mm, force5_50mm, 'color', 'blue')
hold on
plot (newtime5_60mm, newforce5_60mm, 'color', 'red')
% plot (time5_60mm, force5_60mm, 'color', 'red') Plotted line without delay
title ('Combined plot, setup 5')
xlabel('Time [s]')
ylabel('Moment [Nm]')
legend({'50mm' , '60mm'})
xlim([0,35]);
grid on
hold off




Setup6_50mm = xlsread ('Setup6_50mm.XLS');          % Setup 6
time6_50mm = smooth (Setup6_50mm (:,1));
force6_50mm = smooth (Setup6_50mm (:,3));

Setup6_60mm = xlsread ('Setup6_60mm.XLS');
time6_60mm = smooth (Setup6_60mm (:,1));
force6_60mm = smooth (Setup6_60mm (:,3))

timestart6 = 50;                                    % Adjust the time delay
newtime6_60mm = time6_60mm(timestart6:end);
newforce6_60mm = force6_60mm(1:length(newtime6_60mm));

figure
plot (time6_50mm, force6_50mm, 'color', 'blue')
hold on
plot (newtime6_60mm, newforce6_60mm, 'color', 'red')
% plot (time6_60mm, force6_60mm, 'color', 'red') Plotted line without delay
title ('Combined plot, setup 6')
xlabel('Time [s]')
ylabel('Moment [Nm]')
legend({'50mm' , '60mm'})
xlim([0,35]);
grid on
hold off
```

```matlab
Setup7_50mm = xlsread ('Setup7_50mm.XLS');              % Setup 7
time7_50mm = smooth (Setup7_50mm (:,1));
force7_50mm = smooth (Setup7_50mm (:,3));

Setup7_60mm = xlsread ('Setup7_60mm.XLS');
time7_60mm = smooth (Setup7_60mm (:,1));
force7_60mm = smooth (Setup7_60mm (:,3));

timestart7 = 8;                                         % Adjust the time delay
newtime7_60mm = time7_60mm(timestart7:end);
newforce7_60mm = force7_60mm(1:length(newtime7_60mm));

figure
plot (time7_50mm, force7_50mm, 'color', 'blue')
hold on
plot (newtime7_60mm, newforce7_60mm, 'color', 'red')
% plot (time7_60mm, force7_60mm, 'color', 'red') Plotted line without delay
title ('Combined plot, setup 7')
xlabel('Time [s]')
ylabel('Moment [Nm]')
legend({'50mm' , '60mm'})
xlim([0,35]);
grid on
hold off
```
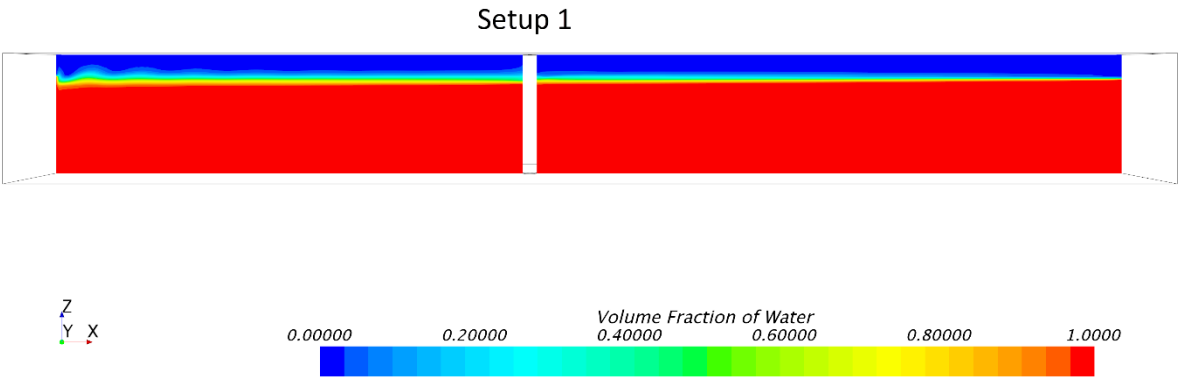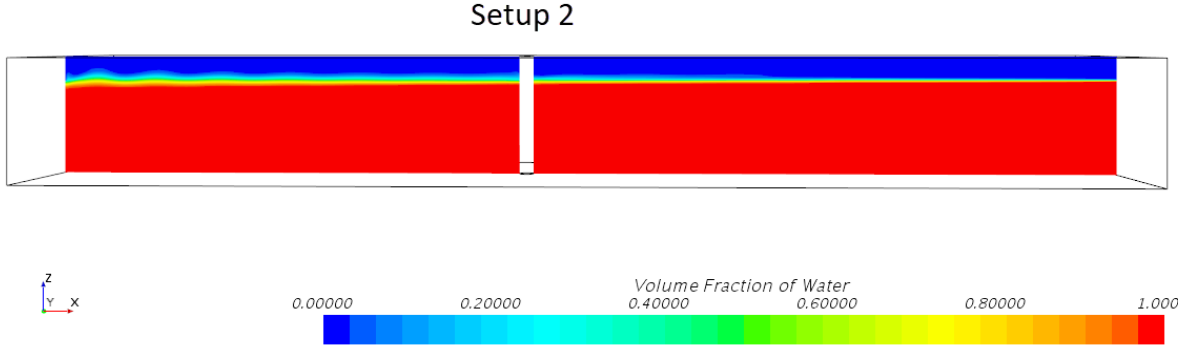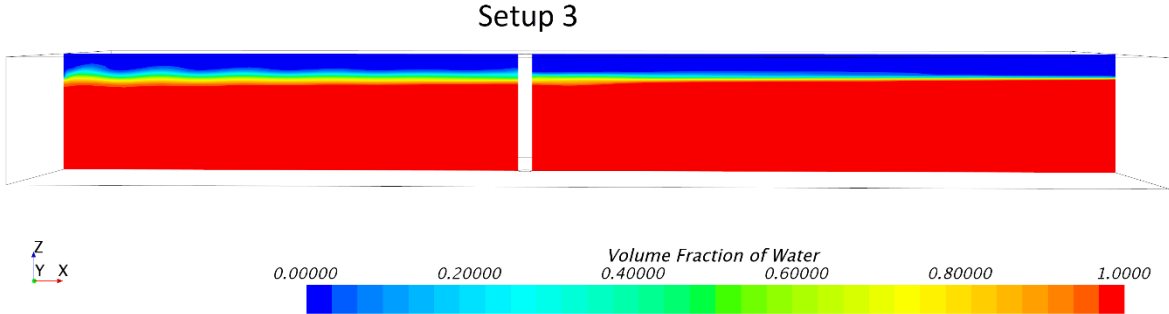
Appendix C – CFD simulation data

Setup 1

Appendix Figure 7 VOF Wave development

Setup 2

Appendix Figure 8 VOF Wave development

Setup 3

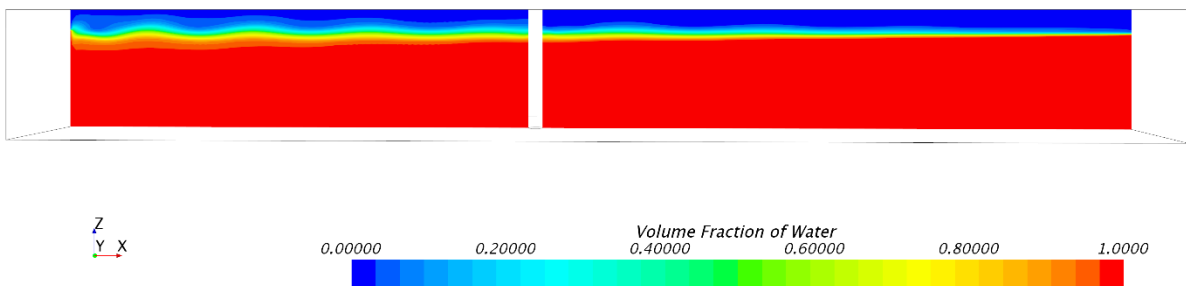**Appendix Figure 9** VOF Wave development

Setup 4
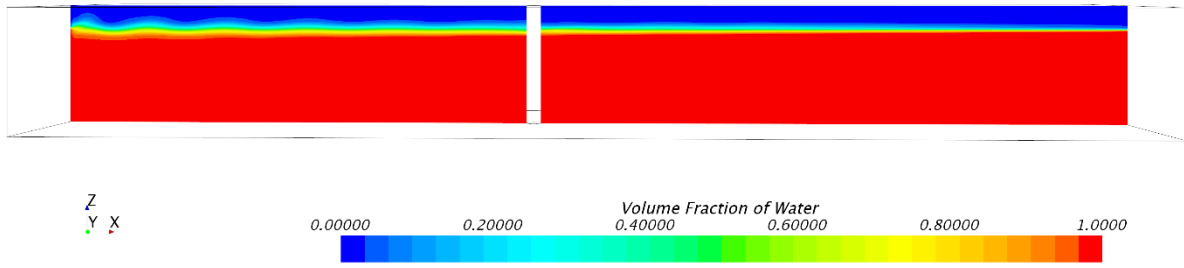
Appendix Figure 10 VOF Wave development
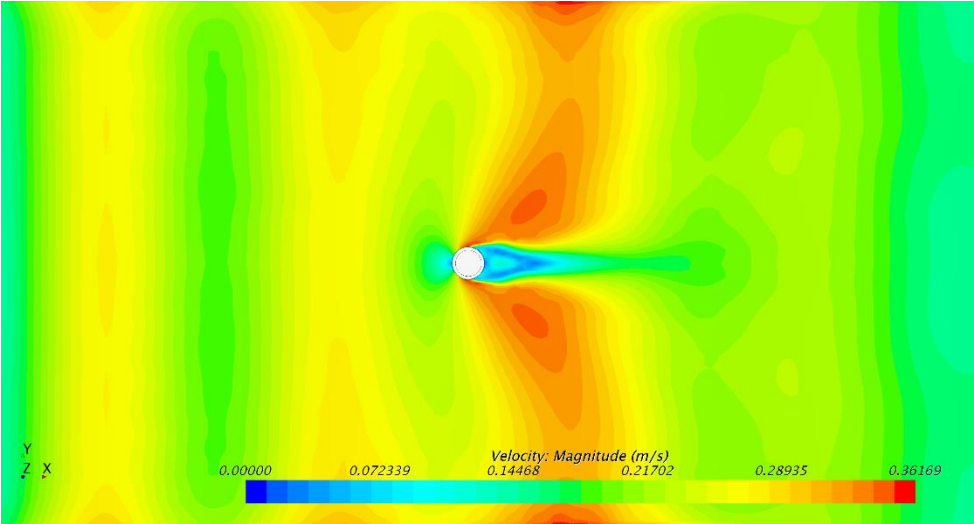

Setup 6
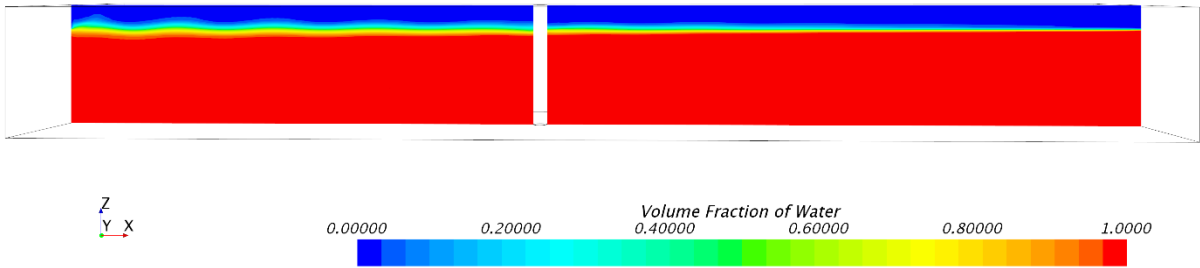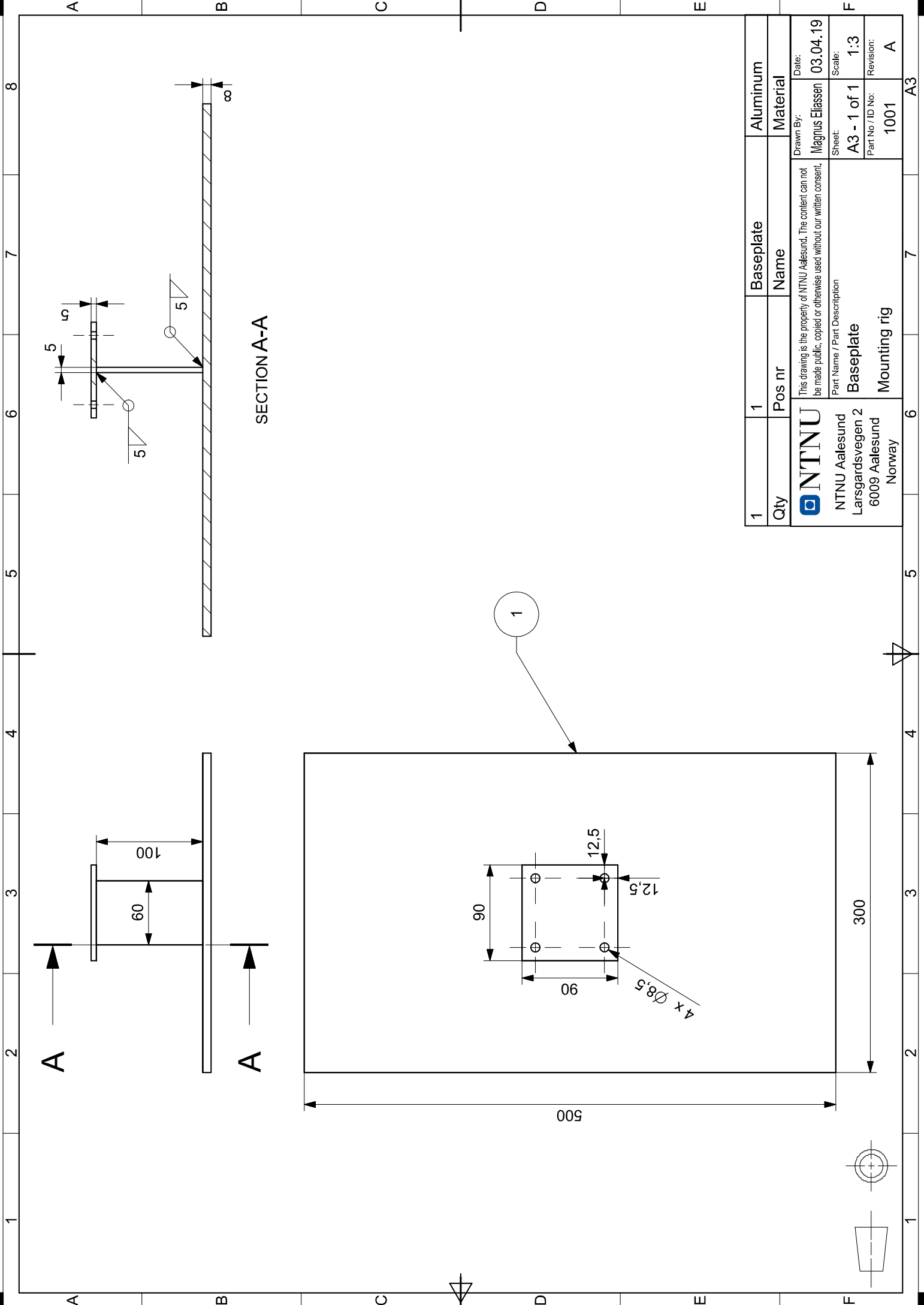

Appendix Figure 11 VOF Wave development

Setup 7

Appendix Figure 12 VOF Wave development

The flow around the cylinder will vary, depending on the parameters of the wave. In Appendix Figure 13, the flow around the cylinder is represented with velocity magnitude. From the figure, it is shown how the cylinder breaks up the wave and divides the flow. The wake behind the cylinder has a reduced flow compared to the surrounding flow. This also occurs right in front of the cylinder, where the flow is "pushing back" resulting in a reduced velocity. The highest velocity is the flow going along the sides of the cylinder and being forced to the sides.

Appendix Figure 13 Velocity flow around the cylinder, setup 6

Appendix D – Machinery drawings

SECTION A-A

8

5

5

5

A

100

60

A

500

300

12,5

12,5

90

90

90

4 x Ø8,5

1

DETAIL B
SCALE 1:2

4 x ⌀8,5

90

12,5

12,5

⌀12

06

006

⌀50

4

5

SECTION A-A

B

All 4 ⌀8,5 holes goes through the plate

2

A

A

2	50mm Cylinder	Aluminum
Pos no	Name	Material

Part Name / Part Description
50mm Cylinder
-

NTNU Aalesund
Larsgardsvegen 2
6009 Aalesund
Norway

Drawn By: Magnus Eliassen
Date: 03.04.19

Sheet: A3 - 1 of 1
Scale: 1:5

Part No / ID No: 1002
Revision: A

A3

1	
Qty	

4 x ⌀8,5

12,5

12,5

90

06

DETAIL B
SCALE 1:2

006

⌀60

6

SECTION A-A

B

All 4 ⌀8,5 holes goes through the plate

5

A

A

5

3

	3	60mm Cylinder	Aluminum
Qty	Pos no	Name	Material

Part Name / Part Description	
60mm Cylinder	
-	

NTNU

NTNU Aalesund
Larsgardsvegen 2
6009 Aalesund
Norway

Drawn By:	Date:
Magnus Eliassen	03.04.19

Sheet:	Scale:
A3 - 1 of 1	1:5

Part No / ID No:	Revision:
1003	A

A3